ENCLOSURE 7

TN Calculation NUH32PHB-0402, Thermal Evaluation of NUHOMS 32PHB Transfer Cask for Normal, Off-Normal, and Accident Conditions

---

AREVA TRANSNUCLEAR INC.	**Form 3.2-1** **Calculation Cover Sheet** TIP 3.2 (Revision 4)	**Calculation No.:**	**NUH32PHB-0402**
		Revision No.:	**0**
		Page: 1 of 62	

DCR NO (if applicable) : N/A	**PROJECT NAME:** NUHOMS® 32PHB System
PROJECT NO: 10955	**CLIENT:** CENG - Calvert Cliff Nuclear Power Plant (CCNPP)

CALCULATION TITLE:

Thermal Evaluation of NUHOMS 32PHB Transfer Cask for Normal, Off Normal, and Accident Conditions

SUMMARY DESCRIPTION:

1) Calculation Summary

This calculation determines the maximum component temperatures of the Calvert Cliff Nuclear Power Plant Onsite Transfer Cask (CCNPP-FC TC) loaded with 32PHB DSC at 29.6 kW without forced convection and also provides the 32PHB DSC shell temperature profiles.

2) Storage Media Description

Secure network server initially, then redundant tape backup

If original issue, is licensing review per TIP 3.5 required?

Yes ☐ No ☒ *(explain below)* *Licensing Review No.:*________________________

This calculation is prepared to support a Site Specific License Application by CCNPP that will be reviewed and approved by the NRC. Therefore, a 10CFR72.48 licensing review per TIP 3.5 is not applicable.

Software Utilized (subject to test requirements of TIP 3.3):	**Version:**
ANSYS	10.0
Calculation is complete: Originator Name and Signature: Venkata Venigalla *[signature]*	Date: 04/08/2010
Calculation has been checked for consistency, completeness and correctness: Checker Name and Signature: Davy Qi *[signature]*	Date: 04/08/2010
Calculation is approved for use: Project Engineer Name and Signature: Kamran Tavassoli *[signature]*	Date: 04/09/10

REVISION SUMMARY

REV.	DESCRIPTION	AFFECTED PAGES	AFFECTED Computational I/O
0	Initial Issue	All	All

TABLE OF CONTENTS

LIST OF TABLES

LIST OF FIGURES

1.0 PURPOSE

This calculation determines the maximum component temperatures of the Calvert Cliff Nuclear Power Plant Onsite Transfer Cask (CCNPP-FC TC) loaded with 32PHB DSC at 29.6 kW without forced convection. It also establishes the maximum time limits for transfer operations of a 32PHB DSC with 29.6 kW heat load in CCNPP-FC TC before initiation of a corrective action such as forced air circulation or refilling the TC/DSC annulus with clean demineralized water.

The CCNPP-FC TC model provides the 32PHB DSC shell temperature distributions for 32PHB DSC/Basket model to be evaluated in Reference [13].

2.0 REFERENCES

1 U.S. Code of Federal Regulations, Part 71, Title 10, "Packaging and Transportation of Radioactive Material".

2 U.S. Code of Federal Regulations, Part 72, Title 10, "Licensing Requirements for the Independent Storage of Spent Nuclear Fuel and High-Level Radioactive Waste".

3 Calvert Cliffs Independent Spent Fuel Storage Installation UPDATED SAFETY ANALYSIS REPORT, Rev.17.

4 Rohsenow, Hartnett, Cho, "Handbook of Heat Transfer", 3rd Edition, 1998.

5 Rohsenow, Hartnett, Ganic, "Handbook of Heat Transfer Fundamentals", 2rd Edition, 1985.

6 ASME Boiler and Pressure Vessel Code, Section II, Part D, "Material Properties", 1998 with 1999 Addenda.

7 ASME Boiler and Pressure Vessel Code, Section II, Part D, "Material Properties", 1992.

8 Perry & Chilton, Chemical Engineers Handbook, 5th Edition, 1973.

9 American Institute of Steel Construction, "AISC Manual of Steel Construction," 9th Edition.

10 ANSYS computer code and On-Line User's Manuals, Version 10.0.

11 Design Criteria Document, "Design Criteria Document (DCD) for the NUHOMS® 32PHB System for Storage", Transnuclear, Inc., NUH32PHB.0101 Rev. 0.

12 Calculation, "NUHOMS® 32P, Finite Element Model, Thermal Analysis", Transnuclear, Inc., 1095-5 Rev. 0.

13 Calculation, "Thermal Evaluation of NUHOMS 32PHB Canister for Storage and Transfer Conditions", Transnuclear, Inc., NUH32PHB-0403, Rev. 0.

14 Calculation, "NUHOMS® 32PHB Weight Calculation of DSC/TC System", Transnuclear, Inc., NUH32PHB-0201, Rev. 0

15 M. Greiner, S. Shin, B. Snyder and R.A. Wirtz, 1995, "Transportation Package Thermal and Shielding Response to a Regulatory Fire", Proc. 6th International High Level Radioactive Waste Management Conference, April 30-May 5, Las Vegas, NV, pp. 538-541.

16 Siegel, Howell, "Thermal Radiation Heat Transfer", 4th Edition, 2002.

17 GESC, NAC International, Atlanta Corporate Headquarters, 655 Engineering Drive, Norcross, Georgia (Engineering Report # NS3-020, Effects of 1300°F on Unfilled NS-3, while Bisco Products, Inc., 11/84).

18 Gregory, et al., "Thermal Measurements in a Series of Long Pool Fires", SANDIA Report, SAND 85-0196, TTC-0659, 1987.

19 Weast, Astle, "CRC Handbook of Chemistry and Physics", 61st Edition, 1980-1981.

20 Calculation, "NUHOMS® 32P – Transfer Cask Structural Analysis", Transnuclear, Inc., 1095-35, Rev. 2.

3.0 ASSUMPTIONS AND CONSERVATISM

The following assumptions and conservatism are considered in the calculation.

3.1 CCNPP-FC TC Model

The 32PHB DSC is located inside the CCNPP-FC TC such that a 0.5" gap exists between the DSC and the bottom cover plate of the TC and 0.75" gap exists between the DSC and the top cover plate of the TC. This reduces the axial heat transfer and maximizes the DSC shell temperature, which in turn result in higher fuel cladding temperature.

The decay heat load is simulated by heat generation distributed uniformly over the basket length of 158" on the homogenized region. The basket is centered axially in the 32PHB DSC. A uniform gap of 0.375" is considered between the basket and the top/bottom ends of the 32PHB DSC. This assumption reduces the axial heat transfer and maximizes the DSC shell temperature, which in turn results in higher fuel cladding temperature.

For the transfer operations in horizontal orientation, the lower halves of the CCNPP-FC TC cylindrical surfaces are not exposed to insolance. No solar heat flux is considered over these surfaces. To remove any uncertainty about the solar impact on the vertical surfaces, the entire surface areas of vertical surfaces are considered for application of the solar heat flux.

During the transfer operation in vertical orientation, the DSC is assumed to be centered within the transfer cask and heat transfer through the slide rails is neglected. Further the top and bottom TC are modeled as adiabatic surfaces with only the outer shell surface dissipating heat to the ambient.

No convection is considered within the cask cavity for conservatism.

The grapple ring is not modeled in the current analysis; it is conservatively replaced with air.

Radiation heat exchange is considered between the 32PHB DSC and the TC inner shell by using the AUX12 processor with SHELL57 elements used to compute the form factors.

The following gaps are considered in the CCNPP-FC transfer cask model:

a) 0.0452" radial gap between the gamma shield and the structural shell.
b) 0.06" axial gap between the top cover plate and the top flange
c) 0.025" radial gap between the top cover plate and the top flange
d) 0.75" radial gap between the bottom cover plate and the bottom end plate
e) 0.0625" axial gap between the various end plates in the DSC.

No gap is considered between the neutron shield and the adjacent shells, since the neutron shield (NS-3) is poured in a controlled manner to avoid air pockets (See 4.7.3.3 of [3]).

The radial gap "a" of 0.0452" between the gamma shield and structural shell is justified in APPENDIX B.

Gaps “b” and “c” between the top cover plate and the top flange account for the thermal resistance between bolted components.

The radial gap “d” of 0.75” between the bottom cover plate and bottom end plate is larger than the nominal gap. This is conservative since the hot gaps at thermal equilibrium would be smaller.

The axial gaps “e” of 0.0625” between the DSC end plates maximizes the radial heat transfer through DSC shell toward the TC to bound the maximum component temperatures conservatively.

For the fire accident conditions the gaps from “a” to “d” are replaced with the adjacent materials to allow heat input into the cask from the fire. The gaps are restored for the post-fire conditions.

3.2 32PHB DSC Model

The assumptions and conservatism considered for 32PHB DSC model are the same as those described in [13], Section 3.0, except those noted below.

During loading operations, the water level in cask/DSC annulus is maintained 12” below the DSC top and is open to atmospheric pressure until the DSC is sealed. The water in the annulus will be observed and replenish as described in [3], Section 5.1.1.3. These operational requirements prevent annulus water from approaching boiling temperature and assure that the DSC shell temperature doesn’t exceed the boiling temperature of water.

Therefore, a conservative DSC shell temperature of the 212°F is used for establishing the initial conditions in the CCNPP-FC TC when the TC is in the vertical orientation and the DSC/TC annulus is filled with water. See APPENDIX C for justification of DSC shell temperature.

4.0 DESIGN INPUT

4.1 Design Load Cases

The following design cases in Table 4-1 are analyzed in this calculation to determine the thermal performance of CCNPP-FC TC with 32PHB DSC at 29.6 kW and without forced convection (FC). The load cases are based on requirements in [11].

Table 4-1 Design Load Cases for 32PHB DSC in CCNPP-FC TC without FC

Case	Operation Condition	Description	Notes	Ambient Temperature	Insolation	Airflow
				[°F]	[Btu/hr-ft^2]	[cfm]
1	Normal	Normal Hot	(3)	104	82	0
2	Normal	Normal Cold	(3)	-8	0	0
3	Off-Normal	Off-Normal Hot	(3)	104	127	0
4	Off-Normal	Off-Normal Cold	(3)	-8	0	0
5	Normal	Vertical Operations, Transient	(1)	100	0	0
6	Off-Normal	Off-Normal Hot, Transient	(1)	104	127	0
7	Accident	Fire Accident	(2)	104/1475/104	127	0

Notes:

1) Initial steady-state conditions with 212°F water assumed in the DSC/TC annulus. At time t=0, the water is drained, no forced air circulation is available, and the system begins to heat up.
2) 15 Minute Fire Transient. 10CFR71. 73 [1] fire criteria used for fire properties with a fire emissivity of 1.0. Initial temperatures taken from transient results at 20 hours in load case # 6 (i.e. the time limit for transfer operations without forced air circulation). Post-fire condition assumes the decomposition of the neutron shield with no forced convection available.
3) Load cases # 1, 2, 3 and 4 are bounded by the Load Case # 6 (See Section 6.0 for justification).

4.2 Major Dimensions in the CCNPP-FC TC Model

Major dimension of 32PHB DSC used in the CCNPP-FC TC model are listed in Table 4-2 below.

All other dimensions are based on nominal dimensions of CCNPP-FC transfer cask drawings listed in DWG NUH32PHB-30-11.

Table 4-2 Major Dimension of 32PHB DSC in CCNPP-FC TC model [14]

DSC Component	Length
	[in]
Bottom End Plates	
Bottom Lead Casing Plate	0.50
Bottom Lead Shielding	4.25
Bottom Cover Plate	1.75
Top End Plates	
Lead Plug Top Casing Plate	0.75
Top Lead Shielding	4.00
Top Inner Cover Plate	1.50
Outer Top Cover Plate	1.25
Cavity Length	158.75(1)
DSC Length (w/o grapple)	172.75
Basket height	158.00

Note 1: 158.63"is the minimum length for DSC the cavity as shown in [14]. However, the nominal length of 158.75" used in this calculation [Nominal Cavity Length = DSC Length (172.75") - Total thickness of the top end plates (7.5") and bottom end (6.5")].

4.3 Thermal Properties of Materials

Materials used in CCNPP-FC TC model are listed in Table 4-3. Thermal properties used in CCNPP-FC TC model are listed in Table 4-4 through Table 4-13 for reference.

Table 4-3 List of Materials in the CCNPP-FC TC Model

Component	Mat # in ANSYS Model	Material
Transfer Cask Properties		
Bottom Cover Plate (1" thick)	101	SA240 Type 304
Bottom End Plate (0.75" thick)	102	SA240 Type 304
Bottom Support Ring	103	SA182 F304N
Bottom Cover NS-3 (3.5" thick)	104	NS-3
Plate for Bottom Cover (0.5" thick)	105	SA240 Type 304
Bottom Castable NS-3 (3.63" thick)	106	NS-3
Bottom Cover Plate (2" Thick)	107	SA240 Type 304
Ram Access Machined Ring	108	SA182 Type F304N
Plate for Top Cover (0.25" thick)	109	SA240 Type 304
Top Cover NS-3 (3" thick)	110	NS-3
Top Cover Plate (3" thick)	111	SA240 Type 304
Inner Shell (0.75" thick)	112	SA240 Type 304
Lead Shielding (Gamma Shield, 4" thick)	113	ASTM B29
Structural Shell (1.5" & 2" thick)	114	SA516 GR70
Top Flange	115	SA182 Type F304N
Neutron Shield Panel (0.25" thick)	116	SA240 Type 304
NSP Support Angle (0.25" thick)	117	SA240 Type 304
Radial Neutron Shield (4" thick)	118	NS-3
Rails (0.12" thick)	119	Nitronic 60 (Effective Properties used. See Section 5.3)
DSC Properties		
DSC Shell	301	SA240 Type 304
DSC Bottom Shield Plug Assembly	302	Effective Properties used, See Section 5.4.2
DSC Top Shield Plug Assembly + Top Outer Cover Plate	303	Effective Properties used, See Section 5.4.1
DSC Helium Gap	304	Helium
DSC Basket	305	Homogenized Region, Effective Properties [See Table 4-10]
Gaps in Model		
Gap Between Bottom Cover Plate and Bottom End Plate	201	Air
Gaps in Grapple Region	202	Air
Gap between the DSC and the TC bottom cover plate/TC top cover plate and also between the Top Flange and TC Top cover plate	203	Air
Gap between the DSC/TC Annulus	206	Air
Gap between Gamma Shield and Structural Shell	205	Air

Table 4-4 Stainless Steel, SA 240, Type 304 / SA 182 Type F304N [6-8]

Temp (°F)	ρ (lb/in^3)	k (Btu/hr-in-°F)	C_p (Btu/lb-°F)
70	0.290	0.717	0.114
100		0.725	0.114
200		0.775	0.119
300		0.817	0.122
400		0.867	0.126
500		0.908	0.128
600		0.942	0.130
700		0.983	0.132
800		1.017	0.132
900		1.058	0.134
1,000		1.100	0.136

Table 4-5 Carbon Steel, SA 516, Gr.70 [7, 9]

Temp (°F)	ρ (lb/in^3)	k (Btu/hr-in-°F)	C_p (Btu/lb-°F)
70	0.284	1.967	0.106
100		1.992	0.110
200		2.033	0.118
300		2.033	0.122
400		2.017	0.128
500		1.975	0.133
600		1.925	0.136
700		1.867	0.143
800		1.808	0.148
900		1.742	0.155
1,000		1.667	0.164

Table 4-6 Gamma Shield, ASTM B29 Lead [5]

Temp (°F)	ρ (lb/in^3)	K (Btu/hr-in-°F)	C_p (Btu/lb-°F)
-279	0.416	1.912	0.028
-189	0.414	1.825	0.029
-99	0.413	1.767	0.030
-9	0.411	1.733	0.030
81	0.409	1.700	0.031
261	0.406	1.637	0.032
441	0.402	1.579	0.033
621	0.398	1.512	0.034

Table 4-7 Castable Neutron Shield, NS-3 [12, 15]

Operation Condition	k	C_p	Density
Normal & Fire Accident	(Btu-in/hr-in^2-°F)	(Btu/lbm-°F)	(lb/in^3)
	0.0407	0.145	0.0637
	k	C_p	Density
Post-Fire Accident	(Btu-in/hr-in^2-°F)	(Btu/lbm-°F)	(lb/in^3)
	0.0114	0.145	0.0605

Table 4-8 Air Thermal Properties [4]

Temperature (K)	Thermal conductivity (W/m-K)	Temperature (°F)	Thermal conductivity (Btu/hr-in-°F)
200	0.01822	-100	0.0009
250	0.02228	-10	0.0011
300	0.02607	80	0.0013
400	0.03304	260	0.0016
500	0.03948	440	0.0019
600	0.04557	620	0.0022
800	0.05698	980	0.0027
1000	0.06721	1340	0.0032

The above data are calculated base on the following polynomial function from [4].

$k = \sum C_i \, T_i$ for conductivity in(W/m-K) and T in (K)

For 250 < T < 1050 K	
C0	-2.2765010E-03
C1	1.2598485E-04
C2	-1.4815235E-07
C3	1.7355064E-10
C4	-1.0666570E-13
C5	2.4766304E-17

Specific heat, viscosity, density and Prandtl number of air are used to calculate heat transfer coefficients in APPENDIX A based on the following data from [4].

$c_p = \sum A_i \, T_i$ for specific heat in (kJ/kg-K) and T in (K)

For 250 < T < 1050 K	
A0	0.103409E+1
A1	-0.2848870E-3
A2	0.7816818E-6
A3	-0.4970786E-9
A4	0.1077024E-12

$\mu = \sum B_i \, T_i$ for viscosity $(N\text{-}s/m^2) \times 10^6$ and T in (K)

For 250 < T < 600 K	
B0	-9.8601E-1
B1	9.080125E-2
B2	-1.17635575E-4
B3	1.2349703E-7
B4	-5.7971299E-11

For 600 < T < 1050 K	
B0	4.8856745
B1	5.43232E-2
B2	-2.4261775E-5
B3	7.9306E-9
B4	-1.10398E-12

$\rho = P / RT$ for density (kg/m^3) with P=101.3 kPa; R = 0.287040 kJ/kg-K; T = air temp in (K)

$\Pr = c_p \, \mu / k$ Prandtl number

Table 4-9 Helium Thermal Conductivity [4]

Temperature (K)	Thermal conductivity (W/m-K)	Temperature (°F)	Thermal conductivity (Btu/hr-in-°F)
300	0.1499	80	0.0072
400	0.1795	260	0.0086
500	0.2115	440	0.0102
600	0.2466	620	0.0119
800	0.3073	980	0.0148
1000	0.3622	1340	0.0174
1050	0.3757	1430	0.0181

The above data are calculated base on the following polynomial function from [4]

$k = \sum C_i\ T_i$ for conductivity in (W/m-K) and T in (K)

For 300 < T < 500 K		for 500< T < 1050 K	
C0	-7.761491E-03	C0	-9.0656E-02
C1	8.66192033E-04	C1	9.37593087E-04
C2	-1.5559338E-06	C2	-9.13347535E-07
C3	1.40150565E-09	C3	5.55037072E-10
C4	0.0E+00	C4	-1.26457196E-13

Table 4-10 Thermal Properties of Homogenized Basket(1) [13]

Temp (°F)	$k_{basket\ rad}$ (Btu/hr-in-°F)	Temp (°F)	$k_{basket,\ axl}$ (Btu/hr-in-°F)	Temp (°F)	$C_{p\ eff}$ (Btu/lbm-°F)	ρ_{eff} (lb/in^3)
315	0.151	100	1.9946	70	0.095	0.131
403	0.160	200	2.0393	100	0.096	
492	0.169	300	2.0760	200	0.098	
581	0.179	400	2.1055	300	0.099	
672	0.189	500	2.1160	400	0.100	
763	0.199	600	2.1228	500	0.101	
855	0.209	700	2.1297	600	0.101	
949	0.218	800	2.1355	700	0.101	
1045	0.224	900	2.1418	800	0.101	
1143	0.227	1000	2.1474	900	0.102	
				1000	0.102	

Note 1: See Appendix D for justification of effective density and specific heat.

Table 4-11 Effective Conductivity of Top Shield Plug and Top Cover Plate
(See Section 5.4.1 for Justification)

Temp (°F)	k_radial (Btu/hr-in-°F)	k_axial (Btu/hr-in-°F)	Cp_eff (Btu/lbm-°F)	ρ_{eff} (lb/in^3)
70	1.243	0.048	0.062	0.352
100	1.241	0.051	0.062	
200	1.246	0.058	0.064	
300	1.247	0.064	0.065	
400	1.268(1)	0.071	0.067	
500	1.254	0.077	0.068	
600	1.250	0.083	0.068	
700	1.249	0.088	0.069	
800	1.245	0.094	0.069	
900	1.244	0.099	0.070	
1,000	1.244	0.104	0.071	

Note: (1) 1.255 Btu/hr-in-°F is conservatively used in the analysis

Table 4-12 Effective Conductivity of Bottom Shield Plug
(See Section 5.4.2 for Justification)

Temp (°F)	k_radial (Btu/hr-in-F)	k_axial (Btu/hr-in-F)	Cp_eff (Btu/lbm-°F)	ρ_{eff} (lb/in^3)
70	1.362	0.062	0.053	0.367
100	1.358	0.065	0.053	
200	1.352	0.074	0.054	
300	1.345	0.082	0.055	
400	1.358	0.090	0.056	
500	1.332	0.098	0.057	
600	1.320	0.105	0.057	
700	1.309	0.112	0.058	
800	1.297	0.119	0.058	
900	1.286	0.126	0.058	
1,000	1.276	0.132	0.059	

Table 4-13 Effective Conductivity of Slide Rail

(See Section 5.3 for Justification)

t_{rail} =	0.12	in
h_contact =	2.7	Btu/hr-in^2-°F
Temp	k_SS304	k_eff
(F)	(Btu/hr-in-°F)	(Btu/hr-in-°F)
70	0.717	0.223
100	0.725	0.224
200	0.775	0.228
300	0.817	0.232
400	0.867	0.236
500	0.908	0.239
600	0.942	0.241
700	0.983	0.244
800	1.017	0.246
900	1.058	0.248
1000	1.100	0.250

4.4 Surface Properties of Materials

The emissivity value of 0.587 is considered for both the DSC shell (stainless steel) and the transfer cask inner shell (stainless steel) in calculation of thermal radiation exchange between these shells [4].

It is assumed that the absorptivity and the emissivity of stainless steel are equal. Solar absorptivity and emissivity of 0.587 are used for the TC outer surfaces [4].

After fire, the cask outer surfaces will be partially covered in soot. Based on [16], emissivity and solar absorptivity of soot are 0.95. The fire accident thermal analysis conservatively assumes a solar absorptivity of 1.0 and an emissivity of 0.9 for the post fire, cool-down period.

4.5 Design Criteria

The design criteria for the TC are established by temperature limits of its temperature sensitive components. These are the temperature of the lead in the gamma shield and the temperature of the NS-3 solid neutron shielding material.

The melting point of ASTM B29 lead used in the gamma shield is approximately 620°F [8].

For design purposes of this application, the long-term, bulk average temperature of the NS-3 material is set to 280 °F [3] or less, and short-term limits for accident conditions should be 1,300 °F or less [17].

The design criteria and evaluation of 32PHB DSC basket for the various load cases shown in Table 4-1 are presented in Reference [13].

5.0 METHODOLOGY

5.1 CCNPP-FC TC Model

A half-symmetric, three-dimensional finite element model of CCNPP-FC transfer cask (TC) is developed using ANSYS Version 10.0 [10] to provide the DSC shell temperature profile for 32PHB DSC model and to determine the maximum component temperatures of the CCNPP-FC TC for various load cases described in Table 4-1.

The model contains the cask shells, cask bottom plate, cask lid, DSC shell, and DSC end plates with a homogenized basket. The 32PHB DSC dimensions correspond to nominal dimensions listed in Table 4-2.

SOLID70 elements are used to model the components including the gaseous gaps. Surface elements SURF152 are used for applying the insolation boundary conditions. Radiation along the gap between DSC and TC inner shell is modeled using AUX12 processor with SHELL57 elements used to compute the form factors.

Decay heat load is applied as a uniform volumetric heat generated throughout the homogenized region of the basket. The volumetric heat generation rate is calculated as

$$q''' = \frac{Q}{\pi\,(D_i/2)^2\,L_b}$$

q''' = Volumetric Heat Generation Rate (Btu/hr-in^3)
Q = decay heat load (Btu/hr) (to convert from kW multiply by 3412.3)
D_i = DSC inner Diameter (in)
L_b = Basket length (in)

The applied decay heat value in the model is listed in Table 5-1

Table 5-1 Decay Heat Load

DSC Type	Heat Load (kW)	Heat Load (Btu/hr)	D_i (in)	L_b (in)	Decay heat Load (Btu/hr-in^3)
32PHB	29.6	101004	66	158	0.1869

For load cases with insolance, the insolance is applied as a heat flux over the TC outer surfaces using average insolence values listed in Table 4-1. The insolance values are multiplied by the surface absorptivity factor to calculate the solar heat flux. The solar heat flux values used in CCNPP-FC TC model are summarized in Table 5-2.

Table 5-2 Solar Heat Flux

Operating Condition	Solar Heat Flux (Btu/hr-ft^2)	Solar Absorptivity (1)	Total solar heat flux (Btu/hr-in^2)
Normal	82	0.587 (2)	0.334
Off-Normal/Accident	127	0.587 (2)	0.518

Note (1): See Section 4.4 for surface properties.

Note (2): Solar absorptivity of stainless steel is taken equal to its emissivity.

Convection and radiation heat transfer from the cask outer surfaces are combined together as total heat transfer coefficients. The total heat transfer coefficients are calculated using free convection correlations from Rohsenow Handbook [4] and are incorporated in the model using ANSYS macros. These correlations are described in APPENDIX A. The ANSYS macros used in this calculation are listed in Section 8.0.

During transfer when the cask in a horizontal orientation, the DSC shell rests on two slide rails in the TC. These rails are flat stainless steel plates welded to the inner shell of the TC. The thickness of the slide rail is 0.12".

The angle between the lower rail and the vertical plane is 18.5 degree. Considering this configuration shown in Figure 5-1, the distance between the centerline of DSC and centerline of the cask are calculated as follows.

$$R_2^2 = R_1^2 + x^2 - 2\,R_1\,x\,Cos(\alpha)$$

With

$R_1 = D_{i,\,TC}/2 - t_{rail}$
$R_2 = D_{o,\,DSC}/2$
$\alpha = 18.5°$
x = Distance between the DSC and TC centerlines (See Table 5-3)
$D_{i,\,TC}$ = Inner diameter of TC (See Table 5-3)
$D_{o,\,DSC}$ = DSC outer diameter (See Table 5-3)
t_{rail} = cask slide rail thickness = 0.12"

The calculated value for x is listed in Table 5-3. In the ANSYS model, the DSC is shifted down by the amount of x in the Cartesian y-direction within the TC cavity.

Table 5-3 Distance between 32PHB DSC and TC Centerline

DSC Type	$D_{i,TC}$ (in)	$D_{o,DSC}$ (in)	R_1 (in)	R_2 (in)	α (degree)	x (in)
32PHB	68	67.25	33.88	33.625	18.5	0.27

The material properties used in the CCNPP-FC TC model are listed in Section 4.0.

The geometry of the TC model and its mesh density are shown in Figure 5-2 to Figure 5-5.

Typical boundary conditions for TC model are shown in Figure 5-6 through Figure 5-7.

5.2 Fire Accident

For the fire accident analysis, a diesel fuel pool of 190" in diameter, which is the approximate length of the TC, is conservatively assumed to engulf the entire cask. A maximum fuel spill of 100 gallons of diesel fuel which is the maximum capacity of both fuel tanks within the tow vehicle is considered in Section 3.3.6 of CCNPP ISFSI USAR [3]. For this postulated fire accident with a conservative volume of 200 gallons of diesel fuel spill, the thickness of the fuel pool would be 1.63". This pool is assumed to burn at a minimum burning rate of 0.15 in/min [18]. The 1.63" thick fuel pool would burn for 11 minutes. For conservatism a 15 minute fire duration is considered in this analysis.

To determine the maximum temperature of TC and DSC shell during the fire accident, a transient fire analysis is performed for duration of 15 minutes using the criteria described in 10CFR71, part 73 [1]. Based on the requirements in 10 CFR 71, part 73 [1], a fire temperature of 1475 °F and a conservative fire emissivity of 1.0 are considered for the fire conditions. Surface emissivity of 0.8 is considered for the packaging surfaces exposed to fire based on 10 CFR 71, part 73 [1]. A bounding forced convection coefficient of 4.5 Btu/hr-ft^2-°F is considered during burning period based on data from reference [18]. The initial conditions for the fire analysis are obtained from the transient results at 20 hours in load case # 6 (See Table 4-1) (i.e. the time limit for transfer operations without forced air circulation).

From Reference [17], when NS-3 material was heated in a furnace to a temperature of 1300°F ± 100°F (50 minutes to get to 1300°F) for a period of one hour, the weight loss from NS-3 was 41 percent. A white smoke started to come out of the furnace at a temperature of 600°F and continued for the duration of the test. At the end of the test, the NS-3 was solid (consisting of inorganic constituents), it did not burn, and was brittle with no mechanical strength. The thermal properties of the NS-3 for the post-fire conditions are obtained from Ref [15] and listed in Table 4-7.

Transient runs are performed for 48 hours after the fire. The results of the transient runs discussed in Section 6.0 show that the maximum temperatures of cask components except for the components on the exterior surfaces of the TC and NS-3 are increasing during post-fire conditions so that the maximum cask component temperatures obtained for steady-state post-fire conditions bound the maximum temperatures of the TC and DSC for fire accident conditions.

The DSC shell temperature profiles from steady state runs will be used to determine the maximum basket component temperatures including the maximum fuel cladding temperature in a separate calculation [13].

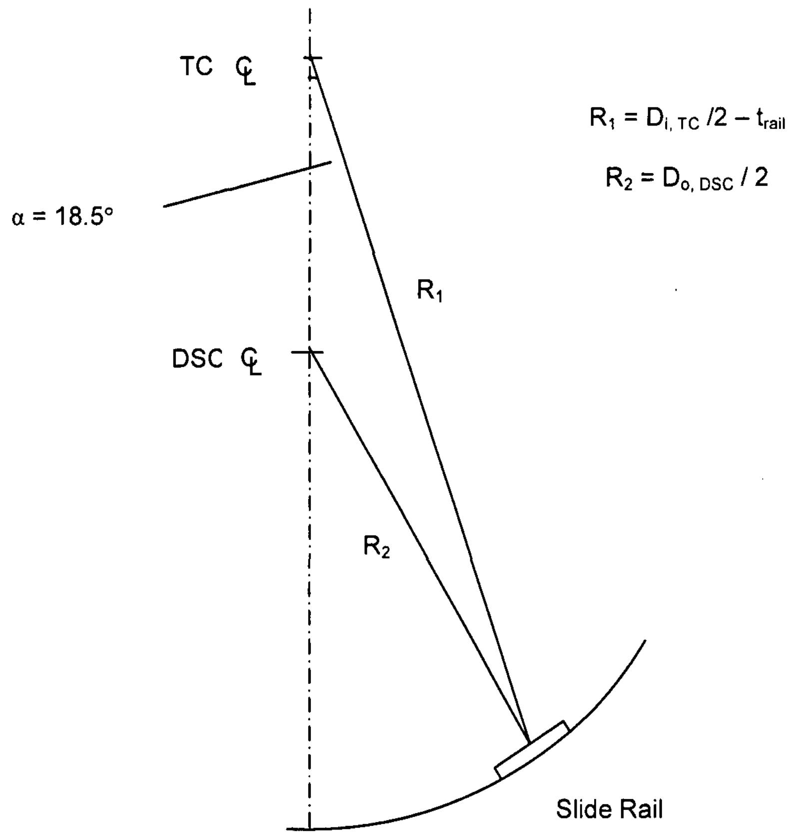

Figure 5-1 Location of 32PHB DSC within CCNPP-FC TC

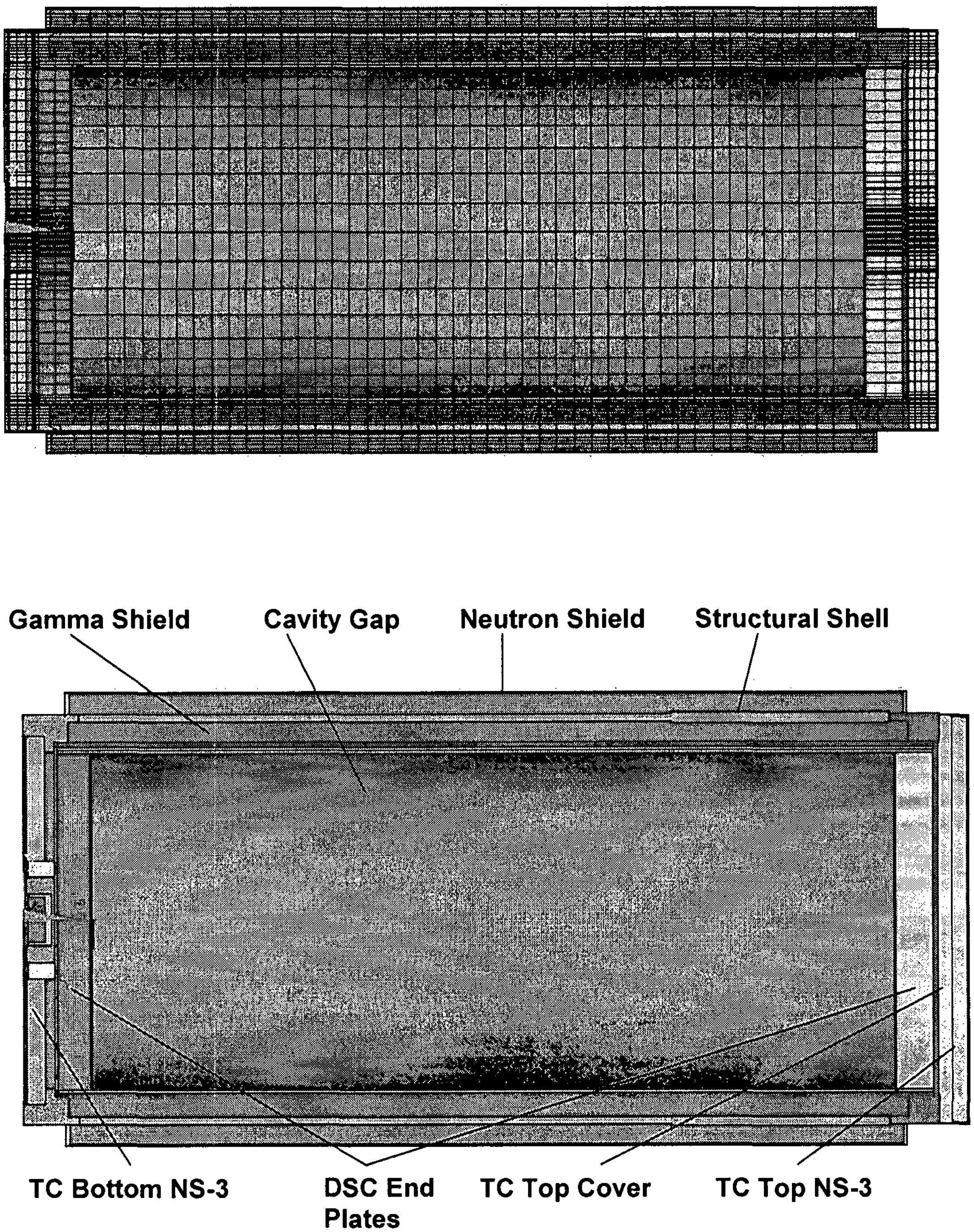

Figure 5-2 Finite Element Model of CCNPP-FC TC with 32PHB DSC

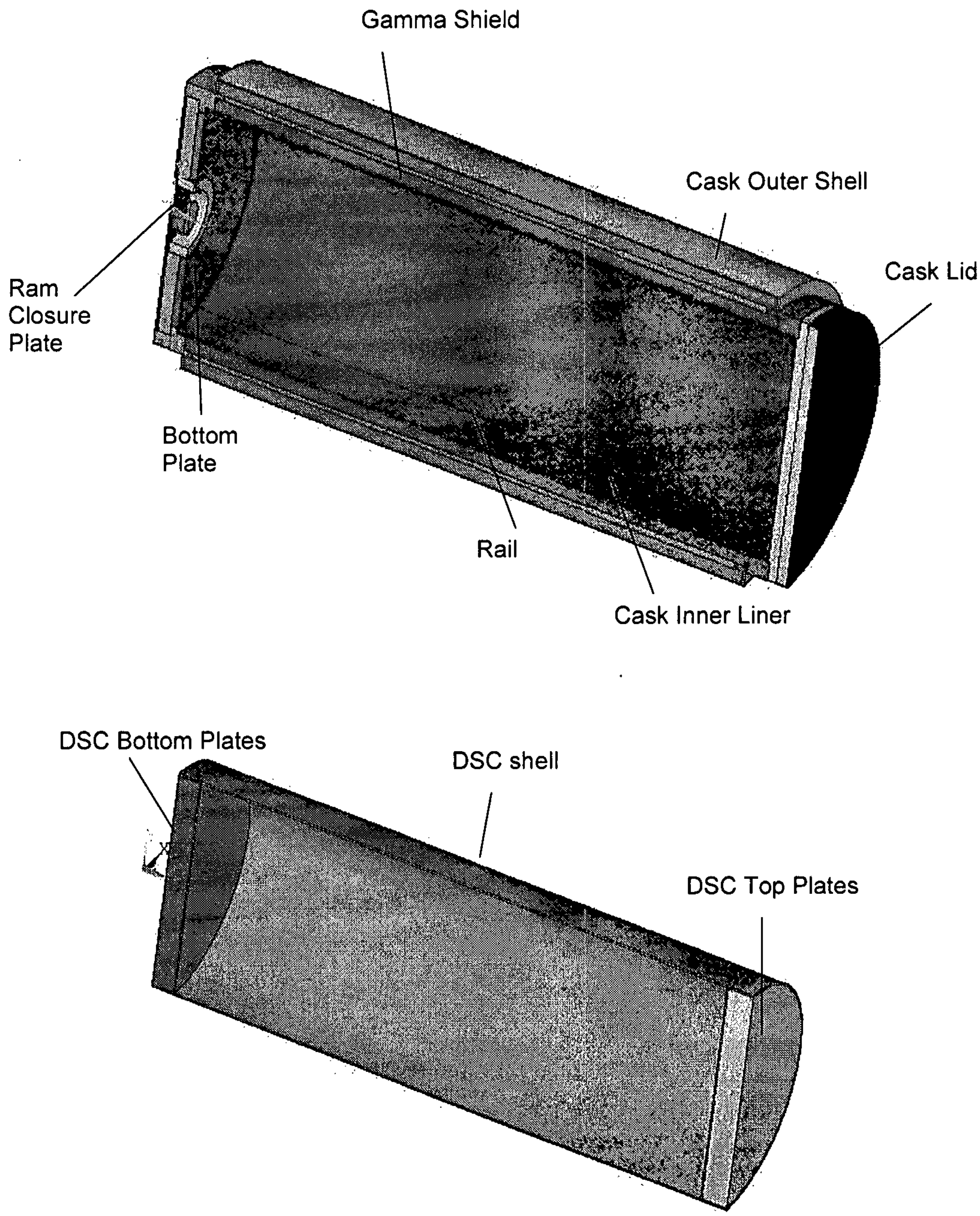

Figure 5-3 CCNPP-FC TC Finite Element Model, Components

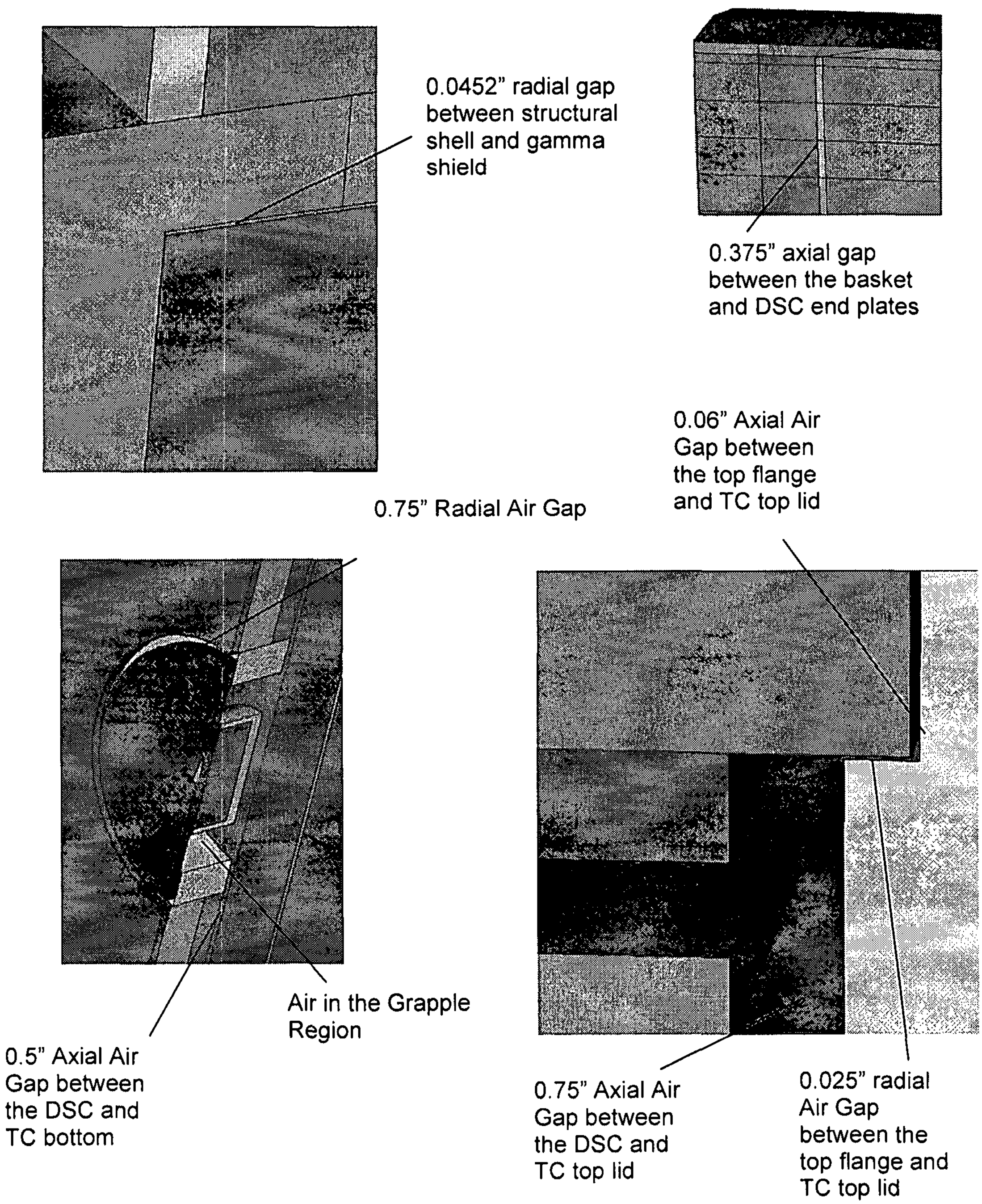

Figure 5-4 Gaps in CCNPP-FC TC Model

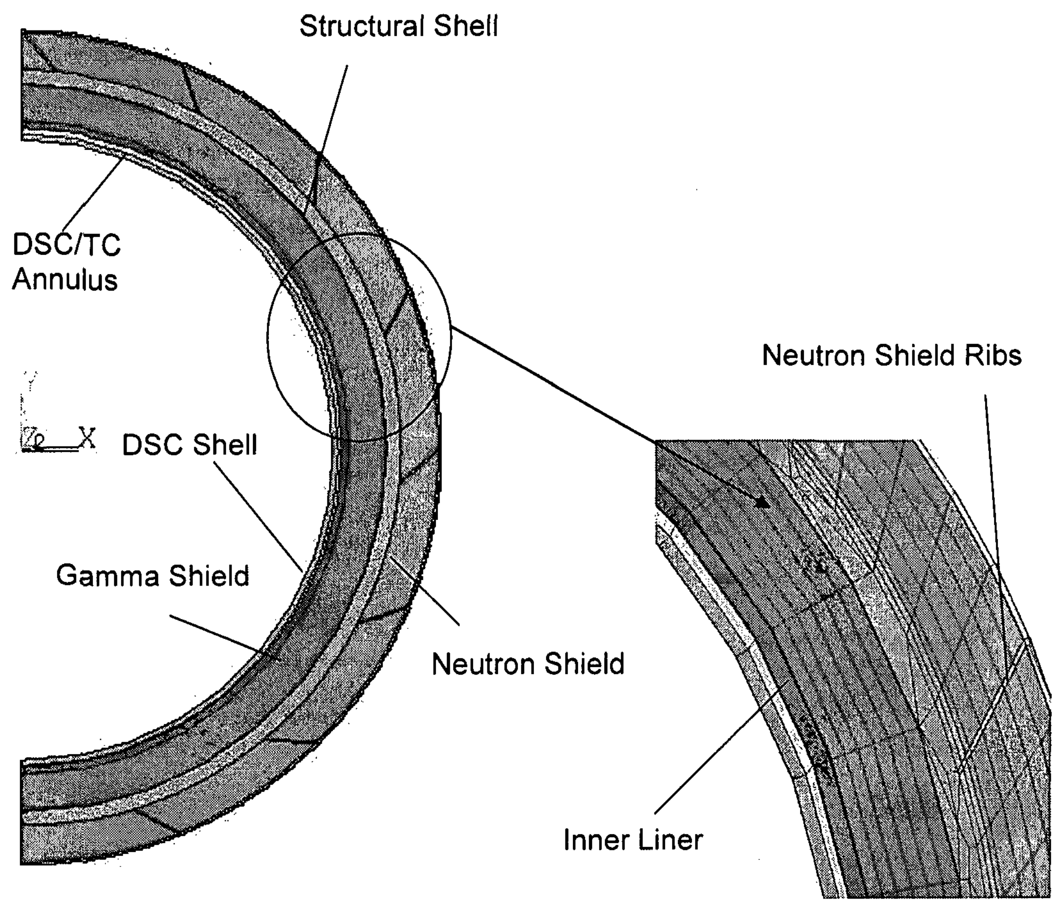

Horizontal TC (DSC is offset)

Figure 5-5 CCNPP-FC TC Finite Element Model, Cross Section

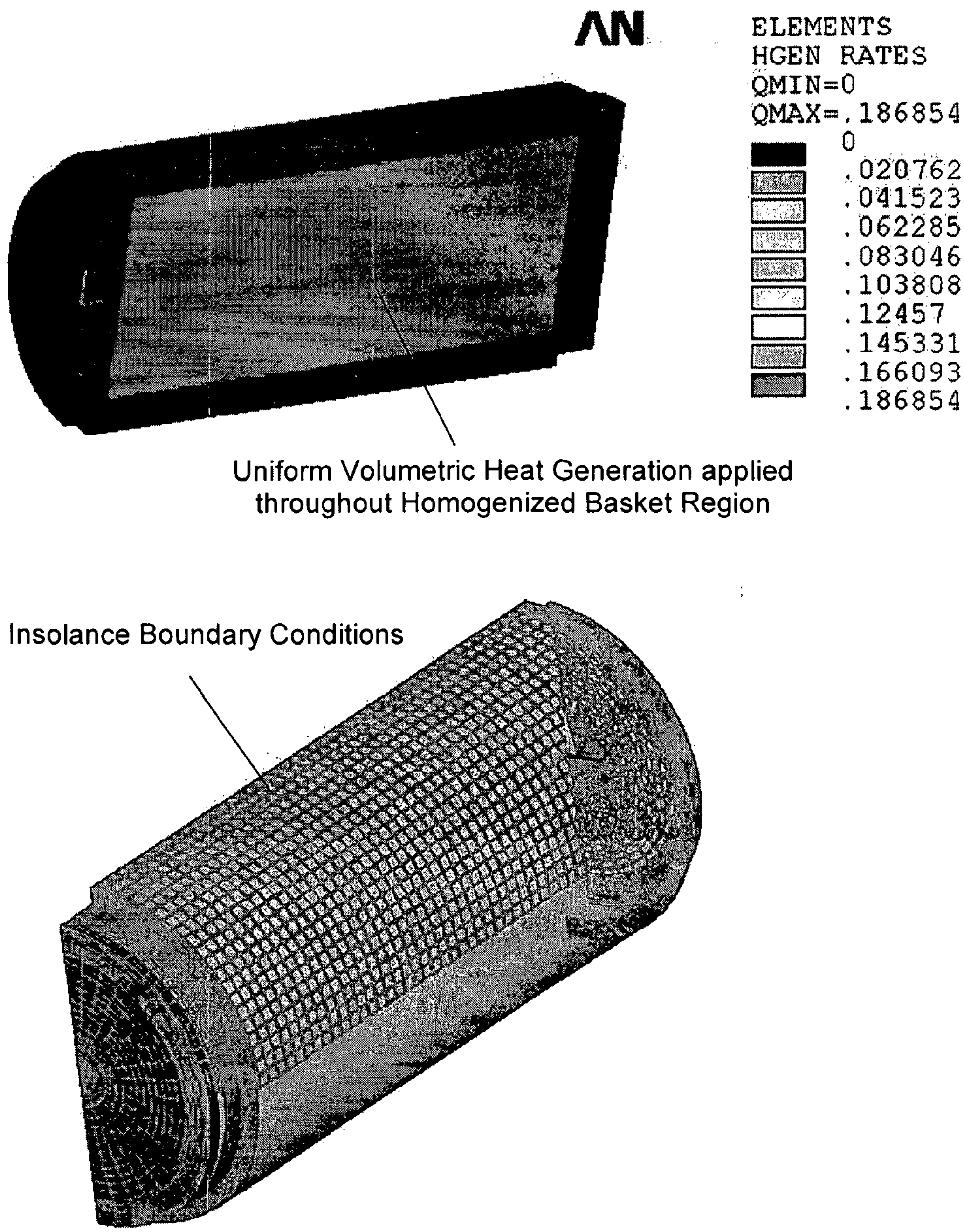

Figure 5-6 Typical Decay Heat and Insolance Boundary Conditions

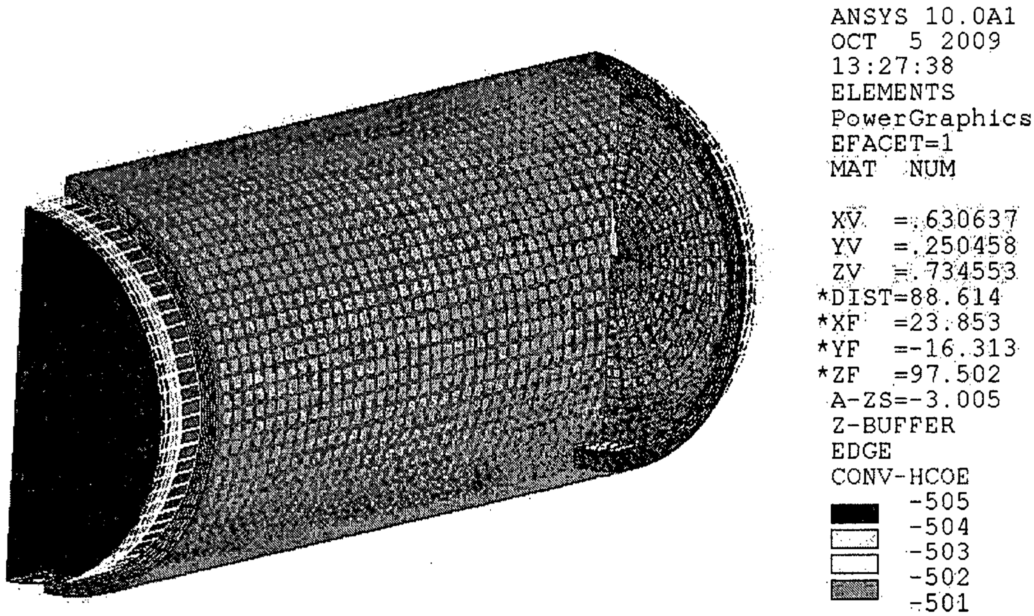

Figure 5-7 Typical Convection and Radiation Boundary Conditions

5.3 Effective Conductivity of Slide Rails

When the TC is in the horizontal orientation, the DSC is supported by the two rails depicted in DWG # BGE-01-3002. Given the weight of a loaded DSC (i.e., > 100,000 lbs) and the surface area of the rails (i.e., 3-inch wide x 167.50-inches long), the contact pressure between a loaded DSC and the rail is in excess of 99 lbs/in^2 (assuming contact with two rails). The thermal resistance between the DSC and the canister rails is assumed to be approximately 2.7 $Btu/hr\text{-}in^2\text{-}^oF$ [per Curve 11, page 4-19, Ref. 5].

The effective conductivity for the rails is calculated based on the following equation and is shown in Table 4-13:

$$k_{eff} = \frac{t_{rail}}{\frac{t_{rail}}{k_{rail}} + \frac{1}{h_{resistance}}}$$

where:

t_{rail} = Thickness of the Rail = 0.12"
k_{rail} = Conductivity of NITRONIC 60 Rails
(Assumed to be SA240 Type 304, See Table 4-4)
$h_{resistance}$ = Contact Resistance = 2.7 $Btu/hr\text{-}in^2\text{-}^oF$

5.4 Effective Thermal Properties of DSC End Plates

The various end plates at the top and bottom of the DSC are modeled as a homogenized region with effective conductivity, density and specific heat.

5.4.1 Top Shield Plug Assembly and Top Cover Plate

The effective properties for the end plates at the top of the DSC are calculated based on the following dimensions

Table 5-4 Thickness and Weights of the Top End Assembly

Component	See Table 1 of Reference [14]			
	Thickness [in]	Volume [in^3]	Weight [lb]	Material
Inner Top Cover Plate	1.5	5,107	1,461	SA240 Type 304
Top Shield Plug	4	13,208	5,429(2)	ASTM B29
Top Casing for Lead(1)	0.75	2,477	708(2)	SA240 Type 304
Outer Top Cover Plate	1.25	4,245	1,214	SA240 Type 304

Note (1): The lead plug side casing plate is neglected.

Note (2): The weight of the Top Shield Plug and Top Casing for Lead are 5428 lbs and 709 lbs, respectively as shown in Table 1 of Reference [14]. The effect on the effective properties due to these changes is negligible.

Effective Thermal Conductivity

Axial air gaps of 0.0625" are considered between each plate shown in the above table. These gaps account for contact resistance and fabrication imperfections between these components and adjacent plates.

The various end plates along with the 0.0625" axial gaps between them built up serial thermal resistances along the axial direction. The effective conductivity through the serial plates is:

$$k_{eff,axial} = \frac{\sum t_{plate}}{\sum \frac{t_{plate}}{k_{plate}}} = \frac{t_{itcp} + t_{tsp} + t_{tcl} + t_{otcp} + (n * t_{gap})}{\frac{t_{itcp}}{k_{itcp}} + \frac{t_{tsp}}{k_{tsp}} + \frac{t_{tcl}}{k_{tcl}} + \frac{t_{otcp}}{k_{otcp}} + \frac{n * t_{gap}}{k_{air,gap}}}$$

where:

t_{itcp}, t_{tsp}, t_{tcl}, t_{otcp}, t_{gap} = thickness of inner top cover plate, top shield plug, top casing for lead , outer top cover plate and air gap, respectively (See Table 5-4).

k_{itcp}, k_{tsp}, k_{tcl}, k_{otcp}, k_{air} = Thermal conductivity of inner top cover plate, top shield plug, top casing for lead, outer top cover plate and air gaps, respectively (See Table 5-4 for materials and Section 4.3 for thermal conductivities).

The various end plates built up parallel thermal resistances along the radial direction. The effective conductivity through the parallel plates is:

$$k_{eff,radial} = \frac{\sum (k_{plate} * t_{plate})}{\sum t_{plate}} = \frac{k_{itcp} * t_{itcp} + k_{tsp} * t_{tsp} + k_{tcl} * t_{tcl} + k_{otcp} * t_{otcp}}{t_{itcp} + t_{tsp} + t_{tcl} + t_{otcp}}$$

where:

t_{itcp}, t_{tsp}, t_{tcl}, t_{otcp} = thickness of inner top cover plate, top shield plug, top casing for lead and outer top cover plate, respectively (See Table 5-4).

k_{itcp}, k_{tsp}, k_{tcl}, k_{otcp} = Thermal conductivity of inner top cover plate, top shield plug, top casing for lead and outer top cover plate, respectively (See Table 5-4 for materials and Section 4.3 for thermal conductivities).

The effective radial and axial thermal conductivities for the top shield plug and top cover plate are shown in Table 4-11.

Effective Density

The effective density of the end plates is calculated as follows:

$$\rho_{eff} = \frac{\sum \rho_{plate} * V_{plate}}{V_{Total}} = \frac{\rho_{itcp} * V_{itcp} + \rho_{tsp} * V_{tsp} + \rho_{tcl} * V_{tcl} + \rho_{otcp} * V_{otcp}}{V_{itcp} + V_{tsp} + V_{tcl} + V_{otcp}}$$

where:

$t_{itcp}, t_{tsp}, t_{tcl}, t_{otcp}$ = thickness of inner top cover plate, top shield plug, top casing for lead and outer top cover plate, respectively (See Table 5-4).

$V_{itcp}, V_{tsp}, V_{tcl}, V_{otcp}$ = Volume of inner top cover plate, top shield plug, top casing for lead and outer top cover plate, respectively (See Table 5-4).

Effective Specific Heat

The effective specific heat for the end plates is calculated as follows:

$$Cp_{eff} = \frac{\sum W_{plate} * Cp_{plate}}{W_{Total}} = \frac{W_{itcp} * Cp_{itcp} + W_{tsp} * Cp_{tsp} + W_{tcl} * Cp_{tcl} + W_{otcp} * Cp_{otcp}}{W_{itcp} + W_{tsp} + W_{tcl} + W_{otcp}}$$

where:

$Cp_{itcp}, Cp_{tsp}, Cp_{tcl}, Cp_{otcp}$ = Specific Heat of inner top cover plate, top shield plug, top casing for lead and outer top cover plate, respectively (See Table 5-4 for materials and Section 4.3 for Cp values).

$W_{itcp}, W_{tsp}, W_{tcl}, W_{otcp}$ = Density of inner top cover plate, top shield plug, top casing for lead and outer top cover plate, respectively (See Table 5-4).

A constant specific heat of 0.030 Btu/lb-°F is used for lead in the calculation of effective specific heat. This is conservative since this decreases the heat capacity.

The effective density and specific heat for the top shield plug and top cover plate are shown in Table 4-11.

5.4.2 Bottom Shield Plug Assembly

The effective properties for the end plates at the bottom of the DSC are calculated based on the methodology described in Section 5.4.1 and the following dimensions

Table 5-5 Thickness and Weights of the Bottom End Assembly

Component	See Table 1 of Reference [14]			
	Thickness	Volume	Weight	Material
	[in]	[in^3]	[lb]	
Inner Bottom Cover Plate	1.75"	6,216	1,778	SA240 Type 304
Bottom Shield Plug	4.25"	14,650	6,021	ASTM B29
Bottom Casing for Lead(1)	0.5"	1,623	464	SA240 Type 304

Note (1): The lead plug side casing plate is neglected.

The effective thermal properties for the bottom end plates of the 32PHB DSC are presented in Table 4-12.

6.0 RESULTS AND DISCUSSION

Due to the high decay heat load of 29.6 kW considered for the NUHOMS® 32PHB system the transfer operations under normal and off-normal steady state conditions listed in Table 4-1 (load case # 1 to 4) are not permitted and operational time limits to complete the transfer operations are established based on the transient thermal analyses performed for normal vertical transfer conditions (load case # 5, Table 4-1) and off-normal hot horizontal transfer conditions (load case # 6, Table 4-1). The time limit established for off-normal hot transfer conditions bounds the time limits for normal hot/cold and off-normal hot/cold conditions.

For the vertical loading transient condition (load cases # 5), the transient begins at steady state with 212°F water in the TC-DSC annulus and the cask is in vertical orientation (i.e. no credit is taken for heat transferred through the rail). At time t= 0, the water in the cask is assumed to be drained, and the cask closure is completed. The TC is assumed to be left inside the fuel building in the vertical position.

For the off-normal hot transient condition (load case # 6), at time = 0, the cask is assumed to be drained, and the cask closure is completed, TC is assumed to be rotated to a horizontal orientation and moved outdoors.

For practical purposes, the time limits for vertical or horizontal transfer operations should be considered after sealing the DSC when the water in the TC/DSC annulus starts to be drained completely.

The NUHOMS® 32PHB system has a provision for forced convection to improve the thermal performance of the system during horizontal transfer conditions and is to be used only as one possible recovery mode if the operational time limits determined for load case # 6 in Table 4-1 are exceeded. The thermal performance of the NUHOMS® 32PHB system with forced air convection will be analyzed in a separate calculation. The forced air convection is not relied on for accident conditions.

Based on the transient thermal analyses a maximum duration of 20 hours is allowed for both the vertical transfer operations (load case # 5) and the off-normal hot horizontal transfer operations (load case # 6). Table 6-1 summarizes the maximum temperatures for the CCNPP-FC TC components and shows that the maximum component temperatures are below the allowable limits for transfer duration of 20 hours.

Figure 6-1 and Figure 6-2 show the temperature distribution of the CCNPP-FC TC and 32PHB DSC for vertical transient conditions.

Figure 6-3 and Figure 6-4 present the temperature profiles for the off-normal horizontal transfer condition at 20 hours for the CCNPP-FC TC and 32PHB DSC.

Table 6-1 Maximum Temperatures of CCNPP-FC TC @ 29.6 kW, NO Forced Air Circulation

Component	Temperature [°F]		
	Vertical Hot Load Case # 5	Off-Normal Hot Load Case # 6	Max. Allowable
	time = 20 hr		
Max. DSC Shell (1)	395	407	---
Inner Shell	279	313	---
Gamma Shield	277	308	620 [8]
Structural Shell	242	263	---
Bulk Avg. Temp of Radial Neutron Shield	201	214	280 [3]
Bulk Avg. Temp of Top Neutron Shield	232	186	280 [3]
Bulk Avg. Temp of Bottom Neutron Shield	240	201	280 [3]
Cask Lid	242	216	---
Cask Outer Shell	238	233	---

(1) The maximum DSC shell temperature is the temperature along the "DSC Shell" as shown in Figure 5-3 and does not include the top and bottom end plates.

Figure 6-5 and Figure 6-6 show the temperature profiles of the DSC and TC at the end of 15 minute fire. Figure 6-7 and Figure 6-8 show the temperature profiles for the steady state post-fire conditions. Table 6-2 presents the maximum component temperature at the end of 15 minute fire, at 48 hours into post-fire and for the steady state post-fire conditions.

Figure 6-9 shows the temperature history of the TC components, DSC Shell and Homogenized Basket during the fire and post-fire conditions. As seen from the figure and Table 6-2, the TC component, the DSC shell and basket temperatures are increasing during the post-fire transient analysis and the maximum temperatures will be achieved under post-fire steady state conditions except for the components on the exterior surfaces of the TC and neutron shield.

Figure 6-10 shows the bulk average temperature history of the NS-3 neutron shield in the TC during and after the fire accident. As seen from the Figure 6-10 the bulk average temperatures of the NS-3 components in the TC increase during the fire and their maximum temperatures are attained at the end of the fire and are listed in Table 6-2.

Table 6-2 Maximum Temperatures of CCNPP-FC TC for Accident Conditions

Component	Temperature [°F]			
	Fire Accident (15 Min. End of Fire)	Post-Fire @ 48 Hours after Fire	Post-Fire Steady State	Max. Allowable
Max. DSC Shell (1)	408	565	656	
Inner Shell	307	492	590	---
Gamma Shield	415	487	585	620 [8]
Structural Shell	352	447	568	---
Bulk Avg. Temp of Radial Neutron Shield	542	295	359	1300 [17]
Bulk Avg. Temp of Top Neutron Shield	640	231	258	1300 [17]
Bulk Avg. Temp of Bottom Neutron Shield	441	258	291	1300 [17]
Cask Lid	910	290	335	---
Cask Outer Shell	1321	332	398	---

(1) The maximum DSC shell temperature is the temperature along the "DSC Shell" as shown in Figure 5-3 and does not include the top and bottom end plates.

The maximum thermal stresses for the TC components except for the bottom cover plate and the ram access penetration ring occur during the hot ambient conditions as noted in Table 4.1.2.1 of [20]. Further the maximum stresses for the bottom cover plate and ram access penetration ring during the cold ambient conditions are significantly below the allowable stress limits. Therefore, the temperature gradients determined for the load case # 6 (Table 4-1, off-normal horizontal hot transfer conditions) are acceptable for the structural evaluation of thermal stresses for the CCNPP-FC TC with 32PHB DSC.

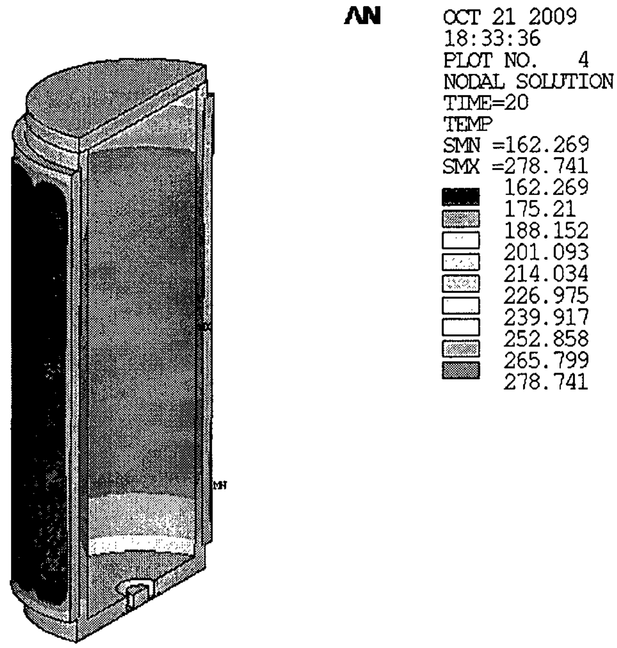

CCNPP-FC-TC with 32PHB, 29.6 kW - Vertical in Fuel Bldg Transient

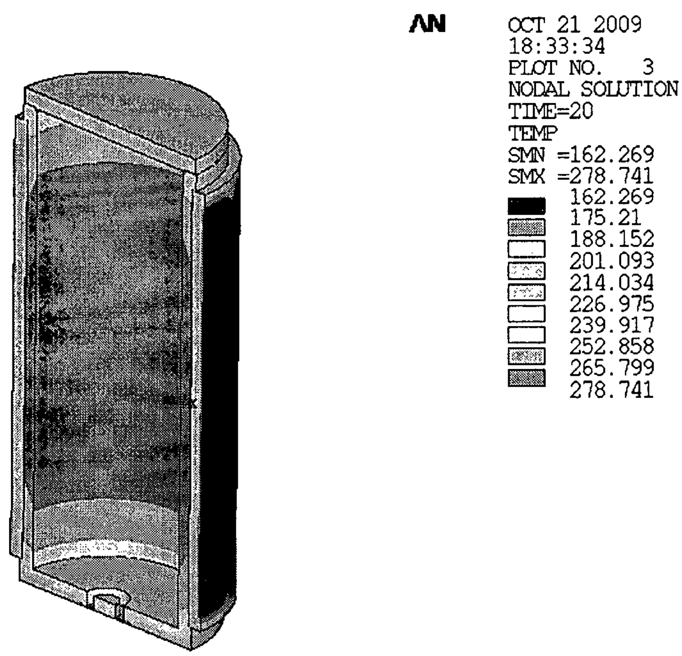

CCNPP-FC-TC with 32PHB, 29.6 kW - Vertical in Fuel Bldg Transient

Figure 6-1 TC Temperature Distribution – Vertical Loading Transient, t = 20 hr @ 29.6 kW, No Insolation, 100°F Ambient (load case # 5)

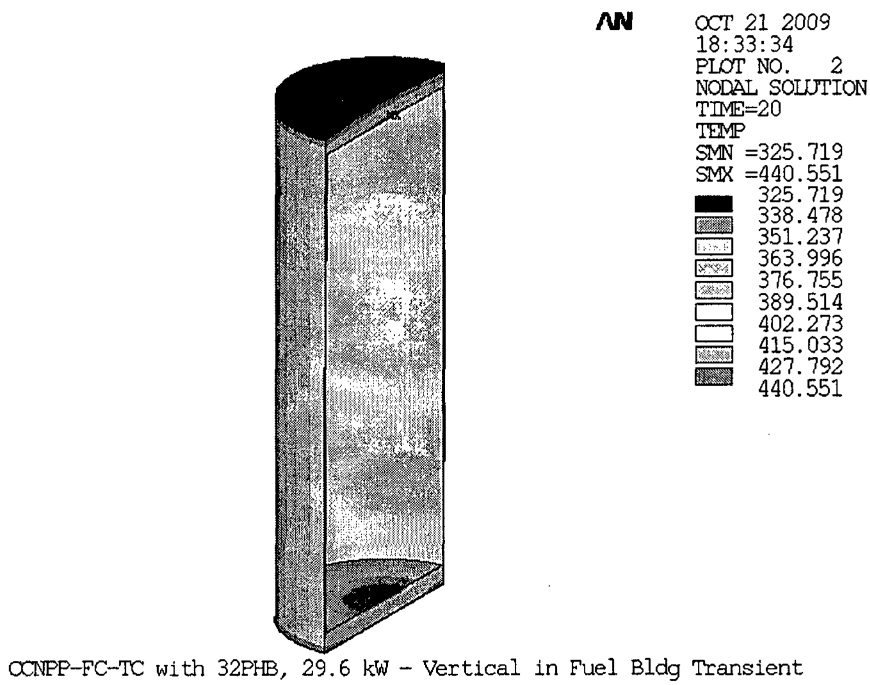

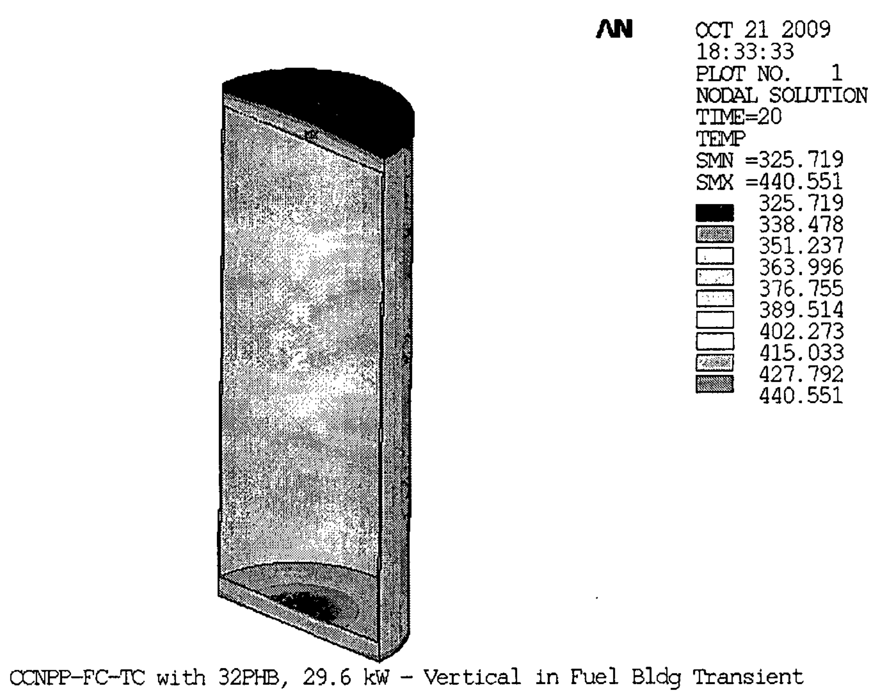

Figure 6-2 DSC Shell Temperature Distribution – Vertical Loading Transient, t = 20 hr @ 29.6 kW, No Insolation, 100°F Ambient (load case # 5)

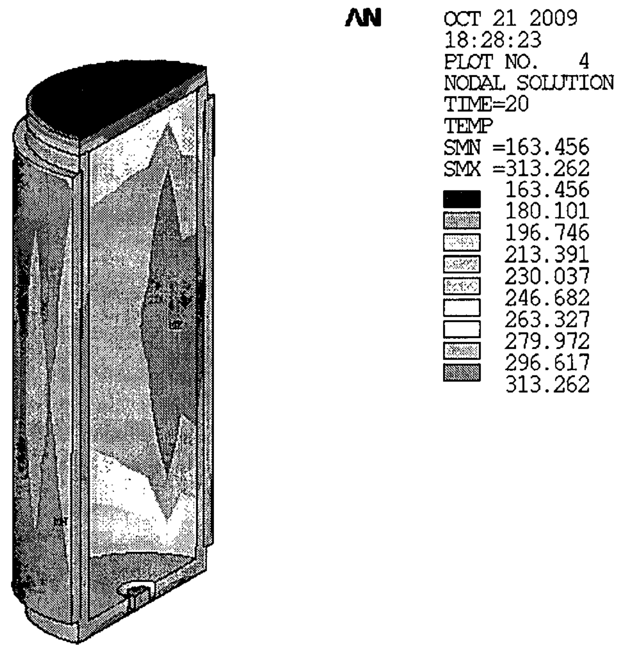

CCNPP-FC-TC with 32PHB, 29.6 kW - Off-Normal Transfer Transient Runs

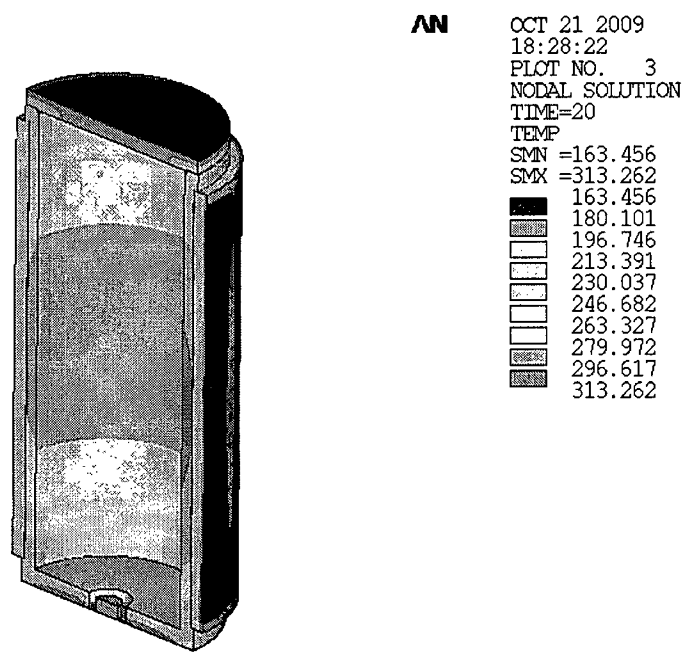

CCNPP-FC-TC with 32PHB, 29.6 kW - Off-Normal Transfer Transient Runs

Figure 6-3 TC Temperature Distribution – Off-Normal Hot Transient, t = 20 hr @ 29.6 kW, 127 Btu/hr-ft^2 Insolation, 104°F Ambient (load case # 6)

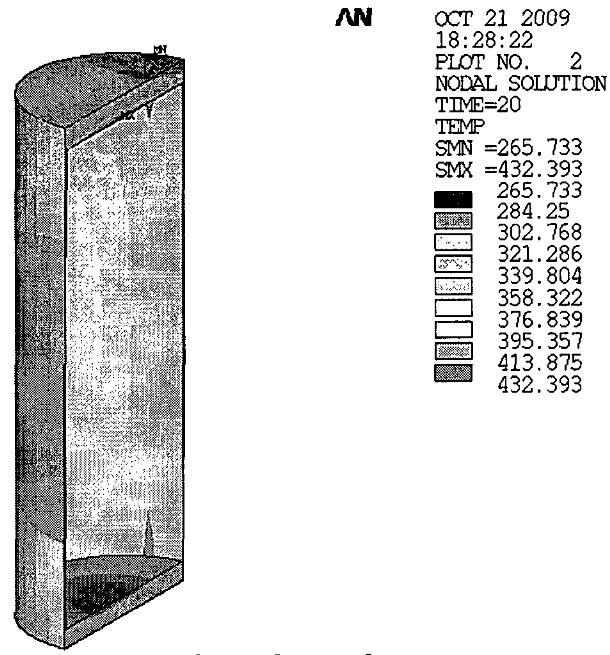

CCNPP-FC-TC with 32PHB, 29.6 kW - Off-Normal Transfer Transient Runs

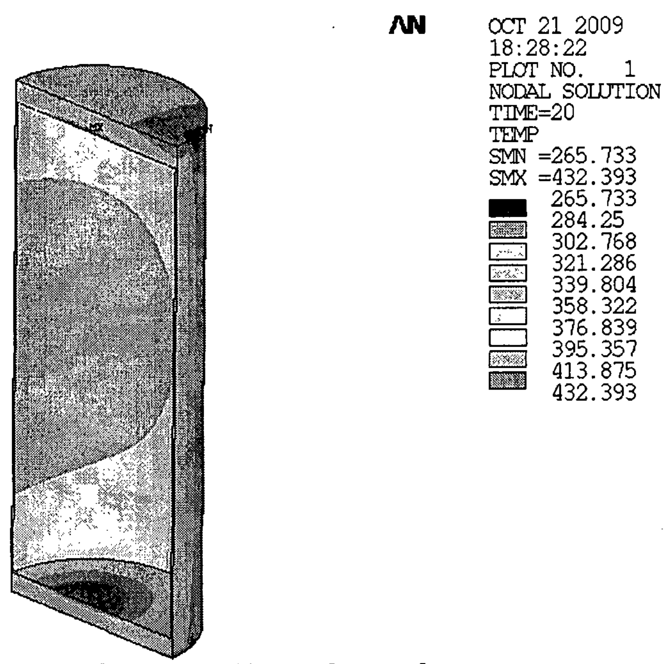

CCNPP-FC-TC with 32PHB, 29.6 kW - Off-Normal Transfer Transient Runs

Figure 6-4 DSC Shell Temperature Distribution – Off-Normal Hot Transient, t = 20 hr @ 29.6 kW, 127 Btu/hr-ft^2 Insolation, 104°F Ambient (load case # 6)

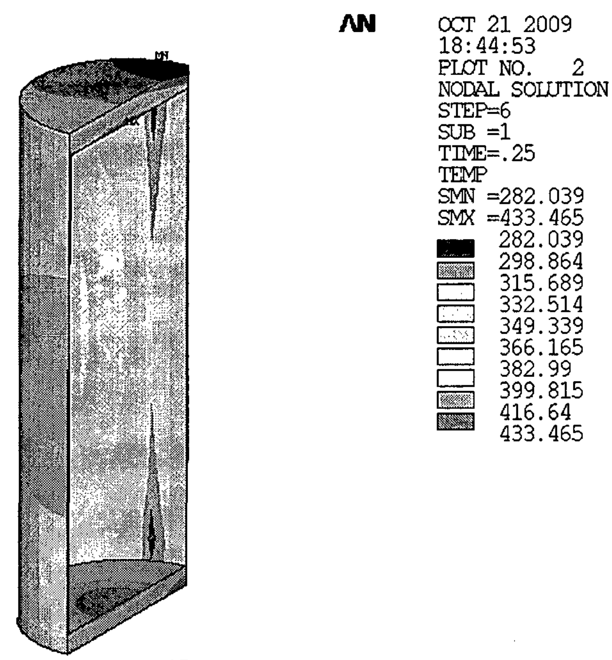

CCNPP-FC-TC with 32PHB, 29.6 kW - 15 Minute Fire Transient Runs

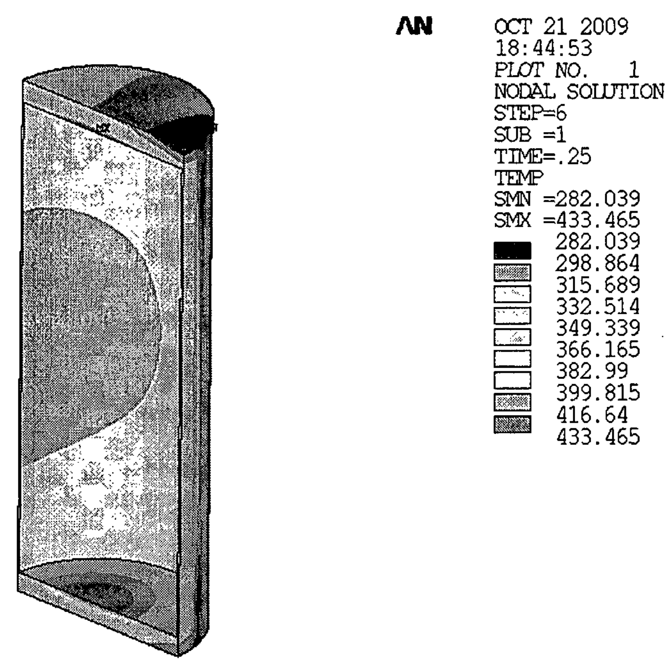

CCNPP-FC-TC with 32PHB, 29.6 kW - 15 Minute Fire Transient Runs

Figure 6-5 DSC Temperature Distribution – Fire Accident, t = 15 min. @ 29.6 kW, 104°F Ambient (load case # 7)

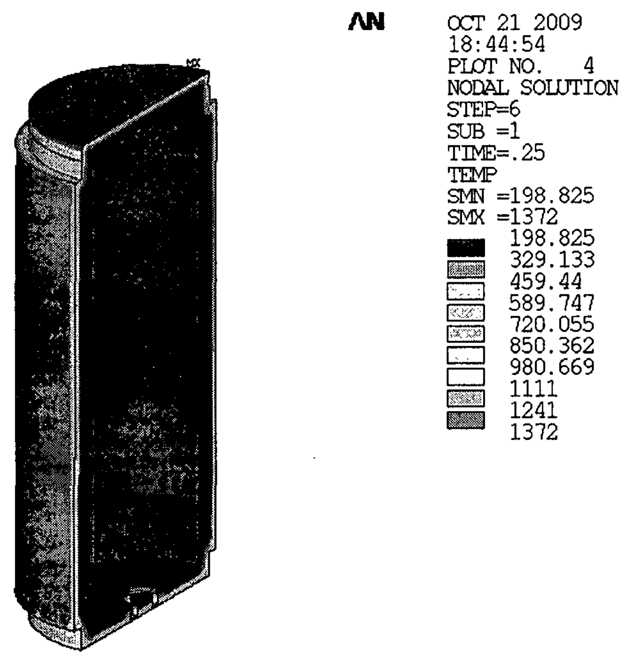

CCNPP-FC-TC with 32PHB, 29.6 kW - 15 Minute Fire Transient Runs

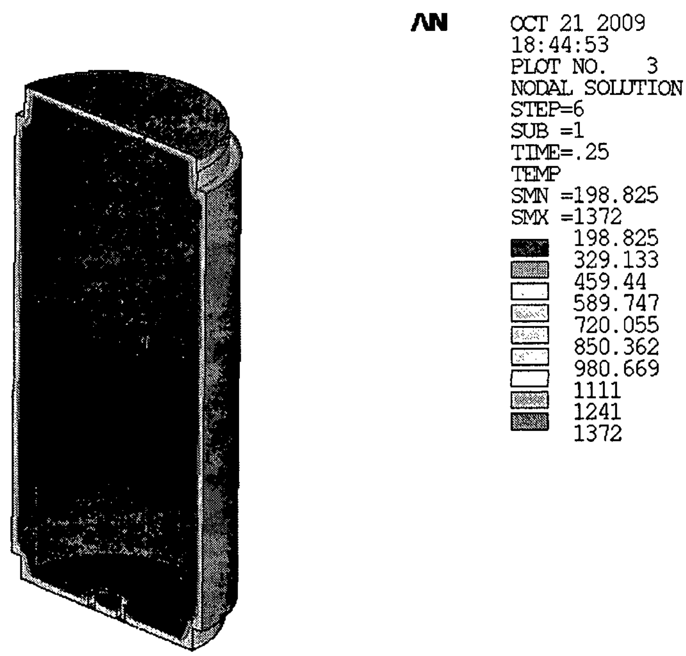

CCNPP-FC-TC with 32PHB, 29.6 kW - 15 Minute Fire Transient Runs

Figure 6-6 TC Temperature Distribution – Fire Accident, t = 15 min. @ 29.6 kW, 104°F Ambient (load case # 7)

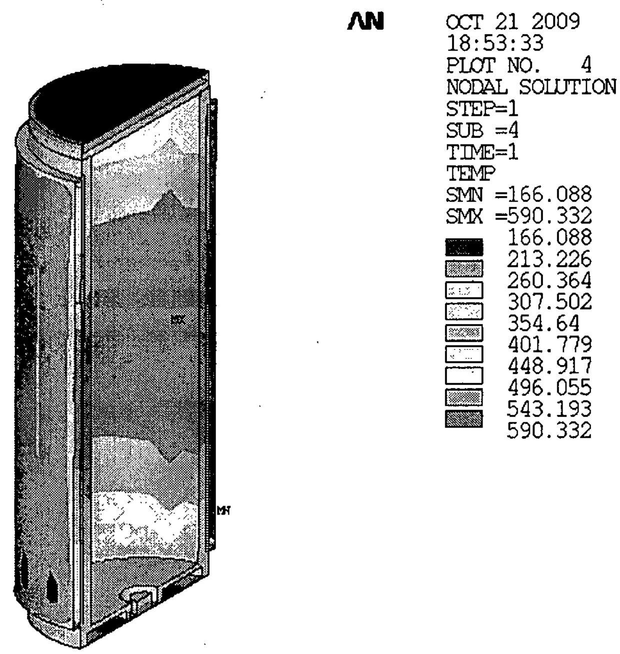

CCNPP-FC-TC with 32PHB, 29.6 kW - Post Fire Steady State

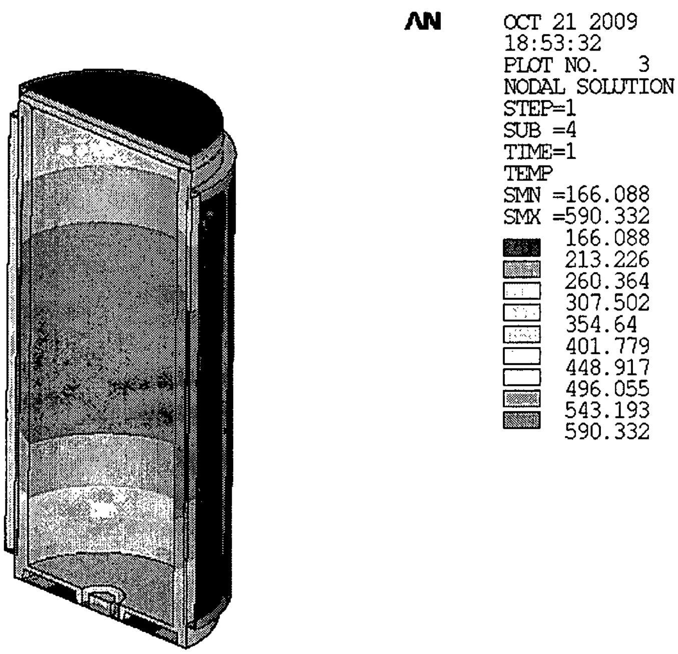

CCNPP-FC-TC with 32PHB, 29.6 kW - Post Fire Steady State

Figure 6-7 TC Temperature Distribution – Post-Fire Accident, Steady State @ 29.6 kW, 127 Btu/hr-ft^2, 104°F Ambient (load case # 7)

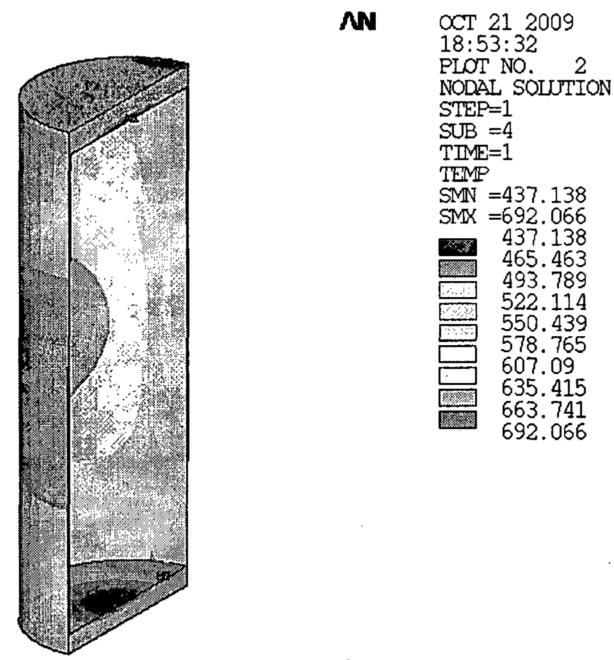

CCNPP-FC-TC with 32PHB, 29.6 kW - Post Fire Steady State

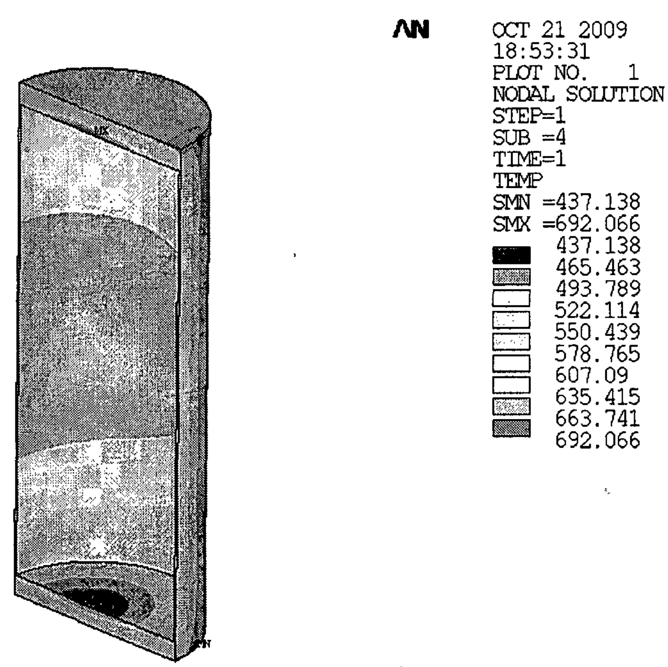

CCNPP-FC-TC with 32PHB, 29.6 kW - Post Fire Steady State

Figure 6-8 DSC Shell Temperature Distribution – Post-Fire Accident, Steady State @ 29.6 kW, 127 Btu/hr-ft^2, 104°F Ambient (load case # 7)

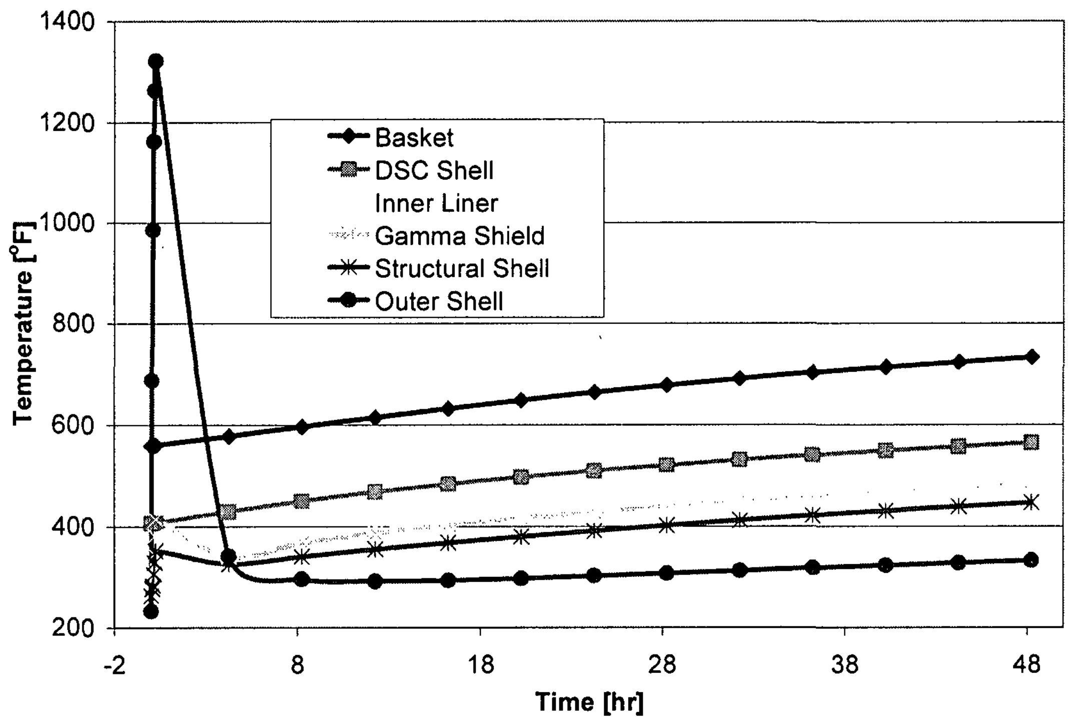

Figure 6-9 Temperature History for Fire and Post-Fire Conditions @ 29.6 kW, 104°F Ambient (load case # 7)

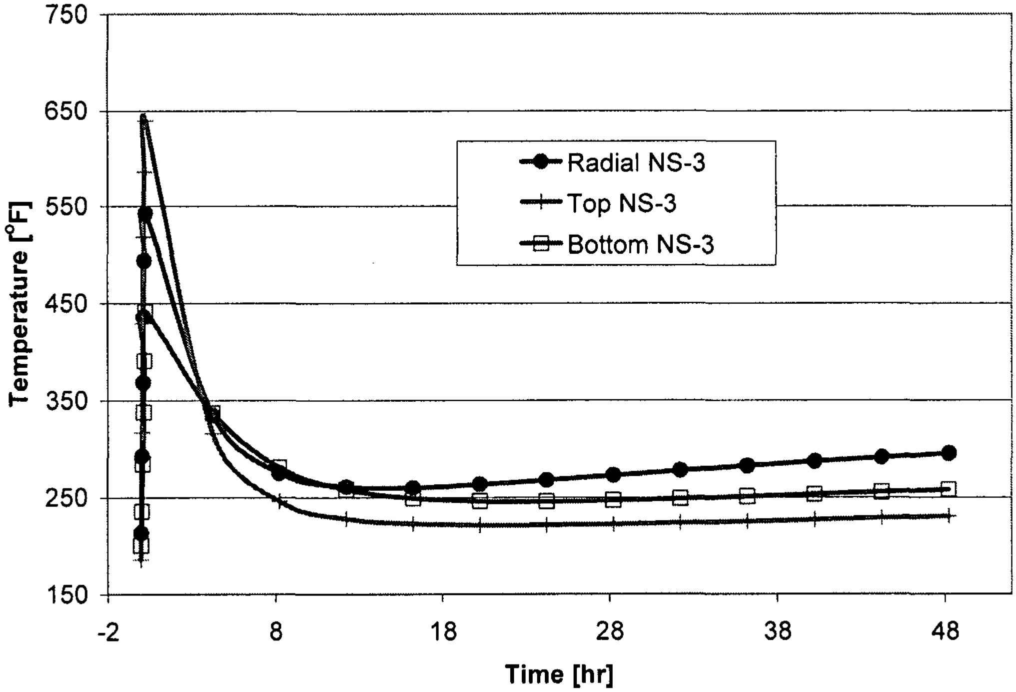

Figure 6-10 Bulk Average Temperature History of NS-3 in TC for Fire and Post-Fire Conditions @ 29.6 kW, 104°F Ambient (load case # 7)

7.0 CONCLUSION

Based on the analyses presented in Section 5.0 and 6.0 the maximum duration for the on-site transfer operations of the CCNPP-FC TC with 32PHB DSC at 29.6 kW is 20 hours. Further a time limit of 20 hours is also established as the maximum duration that the TC can be left in the fuel building in a vertical orientation once the water in the DSC/TC annulus is drained. If the transfer operations exceeds or are expected to exceed the above time limits, corrective actions such as forced air circulation or refilling of the TC/DSC annulus with clean demineralized water should be initiated.

Table 7-1 summarizes the maximum temperatures of the TC components and the DSC shell for vertical hot transient condition in the fuel building and for the off-normal hot horizontal transfer condition after 20 hours.

Table 7-1 Maximum Temperatures of CCNPP-FC TC @ 29.6 kW, NO Forced Air Circulation

Component	Temperature [°F]		
	Vertical Hot Load Case # 5	Off-Normal Hot Load Case # 6 (2)	Max. Allowable
	time = 20 hr		
Max. DSC Shell (1)	395	407	---
Inner Shell	279	313	---
Gamma Shield	277	308	620 [8]
Structural Shell	242	263	
Bulk Avg. Temp of Radial Neutron Shield	201	214	280 [3]
Bulk Avg. Temp of Top Neutron Shield	232	186	280 [3]
Bulk Avg. Temp of Bottom Neutron Shield	240	201	280 [3]
Cask Lid	242	216	---
Cask Outer Shell	238	233	---

(1) The maximum DSC shell temperature is the temperature along the "DSC Shell" as shown in Figure 5-3 and does not include the top and bottom end plates.

(2) For the load cases shown in Table 4-1, Load cases # 1, 2, 3 and 4 are bounded by the Load Case # 6 (off-normal hot horizontal transient transfer operations).

Table 7-2 summarizes the maximum temperatures for the TC components and the DSC shell when subjected to the fire accident conditions along with the time at which they occur.

Table 7-2 Maximum Temperatures of CCNPP-FC TC for Accident Conditions

Components	Time	Maximum Temperature [°F]	Max. Allowable [°F]
Max. DSC Shell (1)	∞	656	---
Inner Shell	∞	590	---
Gamma Shield	∞	585	620 [8]
Structural Shell	∞	568	---
Bulk Avg. Temp of Radial Neutron Shield	End of Fire	542	1300 [17]
Bulk Avg. Temp of Top Neutron Shield	End of Fire	640	1300 [17]
Bulk Avg. Temp of Bottom Neutron Shield	End of Fire	441	1300 [17]
Cask Lid	End of Fire	910	---
Cask Outer Shell	End of Fire	1321	---

(1) The maximum DSC shell temperature is the temperature along the "DSC Shell" as shown in Figure 5-3 and does not include the top and bottom end plates.

As seen the above tables, all design criteria specified in Section 4.5 are herein satisfied.

8.0 LISTING OF COMPUTER FILES

All the runs are performed using ANSYS version 10.0 [10] with operating system "Linux RedHat ES 5.1", and CPU "Opteron 275 DC 2.2 GHz" / "Xeon 5160 DC 3.0 GHz".

A list of the files to create the finite element model of CCNPP-FC with 32PHB DSC is shown in Table 8-1.

Table 8-1 List of Geometry Files

File Name (Input and Output)	Description	Date/Time
CCNPP-FC-TC	Macro to create geometry of CCNPP-FC with 32PHB DSC	08/28/2009 02:41 PM

A summary of ANSYS runs is shown in Table 8-2.

Table 8-2 Summary of ANSYS Runs

Run Name	Description	Date / Time for Output File
32PHB_TC_Initial	Initial conditions of the CCNPP-FC TC with 32PHB DSC in vertical orientation.	10/21/2009 6:16 PM
32PHB_TC_OFN_TRANS	Off-normal hot horizontal transient transfer of the CCNPP-FC TC with 32PHB DSC	10/21/2009 6:28 PM
32PHB_TC_VERT_TRANS	Vertical transient transfer of the CCNPP-FC TC with 32PHB DSC inside the Fuel Building	10/21/2009 6:33 PM
32PHB_TC_ACC_FIRE_INITIAL	Initial conditions for the fire accident analysis	10/21/2009 6:38 PM
32PHB_TC_ACC_FIRE_15MIN	15 Minute Fire Accident Analysis	10/21/2009 6:44 PM
32PHB_TC_ACC_PF	24 Hour Post-Fire analysis	10/21/2009 7:15 PM
32PHB_TC_ACC_NS	Post-Fire Steady State Analysis	10/21/2009 6:53 PM
32PHB_TC_OFN_TRANS_20hr_Map	Temperature profile of 32PHB DSC for off-normal hot transient transfer conditions @ 20 hours	10/21/2009 6:44 PM
32PHB_TC_VERT_TRANS_20hr_Map	Temperature profile of 32PHB DSC for vertical transient transfer conditions @ 20 hours	10/21/2009 6:49 PM
32PHB_TC_ACC_NS_Map	Temperature profile of 32PHB DSC shell for post-fire steady state conditions	10/21/2009 7:00 PM
32PHB_TC_OFN_TRANS_SENS	Sensitivity analysis for effective density and specific heat changes	02/24/2010 3:15 PM

ANSYS macros, and associated files used in this calculation are shown in Table 8-3.

Table 8-3 Associated Files and Macros

File Name	Description	Date / Time
HTOT_HCL.MAC	Total heat transfer coefficients for horizontal cylindrical surface	2/19/2009 12:37 PM
HTOT_VPL.MAC	Total heat transfer coefficients for vertical flat surface	2/19/2009 12:37 PM
HTOT_VCL.MAC	Total heat transfer coefficients for vertical cylindrical surface	2/19/2009 3:52 PM
HTOT_FIRE.MAC	Total heat transfer coefficients for fire	9/12/2008 8:33 PM
32PHBTC_Mat.inp	Material properties for CCNPP-FC Cask	10/21/2009 6:07 PM
32PHBTC_Mat3.inp	Material properties for CCNPP-FC Cask for post-fire steady state	10/21/2009 6:12 PM
32PHB_TC_PP.inp	Macros for Post-Processing Transient Runs	9/16/2009 4:16 PM
32PHB_TC_PP_VERT.inp		9/16/2009 5:48 PM
32PHB_TC_PP_FIRE.inp		9/16/2009 6:48 PM
32PHB_TC_PP_PF.inp		9/22/2009 5:17 PM
Gamma_Gap_32PHB-TC.xls	Spreadsheet to Calculate gamma shield/structural shell gap	01/27/2010 10:17 AM
Gamma_Gap_32PHB-TC-2.xls	Spreadsheet to Calculate gamma shield/structural shell gap for post-fire steady state conditions	01/27/2010 10:17 AM
CCNPP-FC TC-Material Prop.xls	Spreadsheet for material properties used in the analysis	9/21/2009 1:41 PM
Fire History.xls	Spreadsheet for Fire Temperature History Post Processing	10/27/2009 9:59 AM
32PHB_TC_RAD_Horizontal.inp	Macro for Creating Radiation Exchange between the DSC/TC when the TC is in Horizontal Orientation	10/21/2009 4:46 PM
32PHB_TC_RAD_Vertical.inp	Macro for Creating Radiation Exchange between the DSC/TC when the TC is in Vertical Orientation	10/21/2009 4:42 PM

APPENDIX A TOTAL HEAT TRANSFER COEFFICIENTS

Total heat transfer coefficient, h_t, is used to combine the convection and radiation heat transfer together.

$$h_t = h_r + h_c$$

Where,

h_r = radiation heat transfer coefficient (Btu/hr-in^2-°F)
h_c = free convection heat transfer coefficient (Btu/hr-in^2-°F)

The radiation heat transfer coefficient, h_r, is given by the equation:

$$h_r (T_w - T_{amb}) = \varepsilon\, F_{12} \left[\sigma (T_w^{\ 4} - T_{amb}^{\ 4}) \right]$$

$$h_r = \varepsilon\, F_{12} \left[\frac{\sigma (T_w^{\ 4} - T_{amb}^{\ 4})}{T_w - T_{amb}} \right] \quad \text{Btu/hr-in}^2\text{-°F}$$

Where,

ε = surface emissivity
F_{12} = view factor from surface 1 to ambient = 1
σ = 0.1714 $\times 10^{-8}$ Btu/hr-ft^2-°R^4
T_w = surface temperature (°R)
T_{amb} = ambient temperature (°R)

Surface emissivity values are discussed in Section 4.4.

The following equations from Rohsenow handbook [4] are used to calculate the free convection coefficients.

Horizontal Cylinders:

$$Ra = Gr\,\Pr \quad ; \quad Gr = \frac{g\,\beta\,(T_w - T_\infty)\,D^3}{\nu^2}$$

$$Nu_l = \frac{2f}{\ln(1 + 2f / Nu^T)} \quad \text{with}$$

$$Nu^T = 0.772\,\overline{C}_l\,Ra^{1/4} \quad ; \; f = 1 - \frac{0.13}{(Nu^T)^{0.16}} ; \quad \text{with } \overline{C}_l = 0.515 \text{ for gases [4]}$$

$$Nu_t = \overline{C}_t\,Ra^{1/3}$$

$\overline{C}_t = 0.103$ for air with $\Pr \approx 0.71$ [4]

$$Nu = \left[(Nu_l)^m + (Nu_t)^m\right]^{1/m} \quad with \quad m = 10 \quad for \quad 10^{-10} < Ra < 10^7$$

$h_c = \dfrac{Nu\ k}{D}$ (Multiply by 0.1761/144 to convert from W/m²-K to Btu/hr-in²-°F)

with
g = gravitational constant =9.81 (m/s²)
β = expansion coefficient = 1/T (1/K)
T = absolute temperature (K)
ν = kinematic viscosity (m²/s)
D = diameter of the horizontal cylinder (m)
k = air conductivity (W/m-K)

The above correlations are incorporated in ANSYS model via macro "HTOT_HCL.MAC" listed in Section 8.0.

<u>Vertical Flat Surfaces:</u>

$$Ra = Gr\,\Pr \quad ; \quad Gr = \frac{g\,\beta\,(T_w - T_\infty)\,L^3}{\nu^2}$$

$$Nu_l = \frac{2.0}{\ln(1 + 2.0 / Nu^T)} \text{ with}$$

$$Nu^T = \overline{C}_l\, Ra^{1/4} \qquad \text{with } \overline{C}_l = 0.515 \text{ for gases [4]}$$

$$Nu_t = C_t^V\, f\, Ra^{1/3} / \left(1 + 1.4 \times 10^9\, \Pr / Ra\right) \text{ with}$$

$$C_t^V = \frac{0.13\,\Pr^{0.22}}{(1 + 0.61\Pr^{0.81})^{0.42}} \qquad f = 1.0 + 0.078\left(\frac{T_w}{T_\infty} - 1\right)$$

$$Nu = \left[(Nu_l)^m + (Nu_t)^m\right]^{1/m} \quad with \quad m = 6 \quad for \quad 1 < Ra < 10^{12}$$

$h_c = \dfrac{Nu\ k}{L}$ (Multiply by 0.1761/144 to convert from W/m²-K to Btu/hr-in²-°F)

with
g = gravitational constant =9.81 (m/s²)
β = expansion coefficient = 1/T (1/K)
T = absolute temperature (K)
ν = kinematic viscosity (m²/s)
L = height of the vertical surface (m)
k = air conductivity (W/m-K)

The above correlations are incorporated in ANSYS model via macro "HTOT_VPL.MAC" listed in Section 8.0.

Vertical Cylindrical Surfaces:

$$Ra = Gr\,\Pr \quad ; \quad Gr = \frac{g\,\beta\,(T_w - T_\infty)\,L^3}{\nu^2}$$

$$Nu_{l,Plate} = \frac{2.0}{\ln(1 + 2.0 / Nu^T)} \text{ with}$$

$$Nu^T_{Plate} = \overline{C}_l\, Ra^{1/4} \quad \text{with } \overline{C}_l = 0.515 \text{ for gases [4]}$$

$$Nu_l = \frac{\zeta}{\ln(1+\zeta)} Nu_{l,Plate} \text{ with } \zeta = \frac{1.8\,L/D}{Nu^T_{Plate}}$$

$$Nu_t = C^V_t\, f\, Ra^{1/3} / \left(1 + 1.4 \times 10^9\, \Pr / Ra\right) \text{ with}$$

$$C^V_t = \frac{0.13\,\Pr^{0.22}}{(1 + 0.61\,\Pr^{0.81})^{0.42}} \qquad f = 1.0 + 0.078\left(\frac{T_w}{T_\infty} - 1\right)$$

$$Nu = \left[(Nu_l)^m + (Nu_t)^m\right]^{1/m} \quad \textit{with} \quad m = 6 \quad \textit{for} \quad 1 < Ra < 10^{12}$$

$$h_c = \frac{Nu\,k}{L}$$ (Multiply by 0.1761/144 to convert from W/m^2-K to Btu/hr-in^2-°F)

with
g = gravitational constant =9.81 (m/s^2)
β = expansion coefficient = 1/T (1/K)
T = absolute temperature (K)
ν = kinematic viscosity (m^2/s)
L = height of the vertical cylinder (m)
D = Diameter of the Cylinder (m)
k = air conductivity (W/m-K)

The above correlations are incorporated in ANSYS model via macro "HTOT_VCL.MAC" listed in Section 8.0.

APPENDIX B GAMMA SHIELD GAP JUSTIFICATION

A 0.0452" radial air gap is assumed between the gamma shield (lead) and the TC structural shell within the finite element model described in Section 5.0. This air gap is due to the differential thermal expansion of the cask body and the gamma shield during the lead pour.

The following assumptions are made for the verification of the gap:

- The cask body has nominal dimension at 70°F.
- During the lead pour the TC body and lead are at 620°F.
- The inner diameter of the gamma shell (lead) is equal to the outer diameter of the TC inner shell at thermal equilibrium.

The average coefficients of thermal expansion for SA-240 Type 304, SA516 GR70 and lead are listed in Table B-1.

Table B-1 Thermal Expansion Coefficients

Temperature	SA240 Type 304	SA516 GR70
(°F)	α	α
	(in/in-°F) [11]	(in/in-°F) [11]
70	8.46E-06	5.42E-06
200	8.79E-06	5.89E-06
300	9.00E-06	6.26E-06
400	9.19E-06	6.61E-06
500	9.37E-06	6.91E-06
600	9.53E-06	7.17E-06
700	9.69E-06	7.41E-06

Temperature	Lead
(°F)	α
	(in/in-°F) [11]
70	16.07 E-6
100	16.21 E-6
175	16.58 E-6
250	16.95 E-6
325	17.54 E-6
440	18.50 E-6
620	20.39 E-6

The density of lead as a function of temperature is listed in Table .

Table B-2 Density of Lead

Temperature (K)	Density [11] (kg/m^3)	Temperature (°F)	Density (lbm/in^3)
100	11,520	-280	0.4162
150	11,470	-190	0.4144
200	11,430	-100	0.4129
250	11,380	-10	0.4111
300	11,330	80	0.4093
400	11,230	260	0.4057
500	11,130	440	0.4021
600	11,010	620	0.3978

The volume within the "lead cavity" is found by determining the cask body dimensions at 620°F. As no gaps will be present between the molten lead and the cask body, this volume is also equal to the volume of lead at 620°F. The mass of the lead that fills the lead cavity at 620°F is then determined.

The dimensions of the "lead cavity" are calculated based on cask body temperature. A temperature of 305°F is considered for the cask body. This temperature is lower than the maximum cask inner shell temperature shown in Table 6-1. Since the gap size increases at lower temperatures, the above chosen value is conservative. From the mass of the lead and its density at 305°F, the lead volume is determined.

The length of the gamma shield at the TC body temperature is calculated based on thermal expansion coefficients listed in Table B-1. The lead volume is used to determine the maximum size of the air gap adjacent to the lead. See Spreadsheet "Gamma_Gap_32PHB-TC.xls" listed in Table 8-3 for the air gap calculations shown below.

Determination of Lead Mass

$\alpha_{SS304,\,620}$ = 9.56 x 10^{-6} in/in-°F at 620°F (via linear interpolation, Table B-1)
$\alpha_{CS516,\,620}$ = 7.22 x 10^{-6} in/in-°F at 620°F (via linear interpolation, Table B-1)
$\rho_{lead,\,620}$ = 0.3978 lbm/in^3 at 620°F (Table B-2)

R_{in} = inner radius of lead cavity at 70°F= 34.75"
R_{out} = outer radius of lead cavity at 70°F = 38.75"
L_{cavity} = length of lead cavity at 70°F = 165.50"

$R_{in,\,620} = (R_{in})(1+(\alpha_{SS304,\,620})(\Delta T))$ = 34.9328"

$R_{out,\,620} = (R_{out})(1+(\alpha_{CS516,\,620})(\Delta T))$ = 38.9038"

$L_{cavity,\,620} = (L_{cavity})(1+(\alpha_{CS516,\,620})(\Delta T))$ = 166.1570"

$V_{cavity} = V_{lead,\,620} = (\pi)(R_{out,620}^2 - R_{in,620}^2)(L_{cavity,\,620})$ = 153,055.5 in^3

$M_{lead} = (V_{lead,\,620})(\rho_{lead,\,620})$ = 60,878.5 lbm

Determination of Lead Gap

$\alpha_{SS304,\,305}$ = 9.01 x 10^{-6} in/in-°F at 305°F (via linear interpolation, Table B-1)
$\alpha_{CS516,\,305}$ = 6.28 x 10^{-6} in/in-°F at 305°F (via linear interpolation, Table B-1)
$\alpha_{lead,\,620}$ = 20.39 x 10^{-6} in/in-°F at 620°F (via linear interpolation, Table B-1)
$\alpha_{lead,\,305}$ = 17.38 x 10^{-6} in/in-°F at 305°F (via linear interpolation, Table B-1)
$\rho_{lead,305}$ = 0.4048 lbm/in^3 at 305°F (via linear interpolation from Table B-2)

$R_{in,\,SS304,\,305} = (R_{in})(1+(\alpha_{SS304,\,305})(\Delta T))$ = 34.8236"

$R_{out,\,CS516,\,305} = (R_{out})(1+(\alpha_{CS516,\,305})(\Delta T))$ = 38.8072"

$L_{lead,\,305} = (L_{cavity,\,620})/[1+(\alpha_{\,lead,620})(620 - 70)]*(1+(\alpha_{\,lead,305})(305 - 70))$
$= 164.9855"$

$V_{lead,\,305} = M_{lead} / \rho_{lead,\,305} = 150{,}391.8 \text{ in}^3$

Since $R_{in,SS304,\,305} = R_{in,\,lead,\,305}$, then :

$V_{lead,305} = (\pi)(R_{out,\,lead,305}{}^2 - R_{in,\,SS304,\,305}{}^2)(L_{lead,\,305})$

It gives:

$R_{out,\,lead,\,305} = 38.7664"$

Air gap = $R_{out,\,CS516,\,305} - R_{out,\,lead,\,305} = 38.8072 - 38.7664 = 0.0408"$

The assumed air gap of 0.0452" is larger than the above calculated gap. Therefore, using a gap of 0.0452" is conservative to maximize the 32PHB DSC shell temperature.

Based on the above methodology, the air gap is recomputed for the post-fire steady state analysis based on a temperature of 590°F for the cask body. This temperature is the maximum cask inner shell temperature shown in Table 6-2. The computed air gap between the lead and the structural shell is 0.004". To account for the effect in the reduction of the computed air gap between the gamma shield and structural shell from 0.0412" to 0.004", the effective conductivity of air in the region is increased by a factor of 4. This factor of 4 corresponds to an air gap of 0.011" (0.0452/4 = 0.0113") and is therefore conservative for the post-fire steady state conditions.

APPENDIX C DSC SHELL TEMPERATURE

During the handling and vacuum drying operations, the DSC outer shell is in contact with water in annulus between the DSC and the transfer cask. The annulus is open to atmospheric pressure.

To bound the problem, it can be assumed conservatively that the total heat load from the assemblies flows to water in the annulus and no heat dissipation to ambient occurs. As long as the DSC shell is in contact with water, the decay heat will be used to evaporate and eventually boil the water in annulus. The water bulk temperature remains constant at 212°F (100°C) if water starts to boil.

The following calculation shows that the maximum allowable heat load for 32PHB DSC (29.6 kW [11]) is not adequate to boil the water in annulus. Therefore, the maximum bulk temperature for water in annulus is bounded by boiling temperature of 212°F (100°C).

Observations show that the hot surface temperature in contact with boiling water is typically 10-15°C higher than the boiling temperature for heterogeneous nucleation process [4, page 15.9]. The temperature gradient between the hot surface and the boiling water is defined as ΔT_{sat}.

$\Delta T_{sat}. = (T_w - T_{sat}) \geq 10$ to 15°C (C.1)

T_w = hot surface temperature (°C)
T_{sat} = saturated water temperature = 100°C at atmospheric pressure

Under boiling water conditions, ΔT_{sat} can be calculated using the following correlation from [4, page 15.46].

$$\Delta T_{sat} = C_{SF}\left[\frac{q_{DSC}''}{\mu_l\, i_{lg}}\sqrt{\frac{\sigma}{g(\rho_l-\rho_g)}}\right]^{0.33}\left[\frac{\mu_l\, i_{lg}}{k_l}\right] \qquad \text{(C.2)}$$

C_{SF} = liquid/surface constant = 0.013 [4]
q_{DSC}'' = heat flux from hot surface of one fuel rod = 1320 W/m^2 (see below)
μ_l = dynamic viscosity of saturated water = 2.79E-4 N.s/m^2 [4]
i_{lg} = latent heat of vaporization = 970.3 Btu/lbm [4] = 2.257E6 J/kg
σ = surface tension of water = 0.059 N/M [4]
g = gravity constant = 9.8 m/s^2 [4]
ρ_l = density of saturated water = 958 kg/m^3 (v_l = 1.0435E-3 m^3/kg [19])
ρ_g = density of saturated steam= 0.598 kg/m^3 (v_g = 1.673 m^3/kg [19])
k_l = conductivity of saturated water = 0.68 W/m-K [4]

All the properties are at 100°C.

The heat flux from DSC outer shell (q_{DSC}") is calculated as follows.

$$q_{DSC}" = \frac{Q}{\left(\pi\, OD_{DSC}\; L_{ann}\right)} = 1320\ \mathrm{W/m^2} \qquad \text{(C.3)}$$

Q = maximum heat load per DSC = 29.6 kW [11]

OD_{DSC} = Outer DSC shell diameter = 67.25" [11] = 1.708 m

L_{ann} = water height in annulus = DSC height -12" = 176.50 [14, Drawing NUH32PHB-30-1]-12"
= 164.5" = 4.178 m

It is assumed that approximately 12" of water is drained from the DSC top before the welding operation is started [3, Section 5.1.1.3].

Using q_{DSC}" in equation (C.2) gives the ΔT_{sat} for annulus.

$$\Delta T_{sat,ann} = 2.1°\mathrm{C} \qquad \text{(C.4)}$$

$\Delta T_{sat,ann}$ is much lower than the required temperature gradient of 10 to 15°C to boil the water. It concludes that no boiling will occur within the annulus between the DSC shell and transfer cask.

APPENDIX D SENSITIVITY OF THE EFFECTIVE DENSITY AND SPECIFIC HEAT OF THE HOMOGENIZED BASKET

This section presents a sensitivity analysis of the maximum temperatures in the CCNPP-FC TC to the changes in the effective density and specific heat of the homogenized basket considered in the transient analysis.

During the design process of the 32PHB DSC system, the weight of the fuel assembly is decreased which affects the effective specific heat and density of the homogenized basket considered in this calculation and shown in Table 4-10. The updated effective specific heat and density of the homogenized basket used in this appendix from [13] are listed in Table D-1.

Table D-1 Effective Density and Specific Heat [13]

Temp (°F)	$C_{p\ eff}$ (Btu/lbm-°F)	ρ_{eff} (lb/in^3)
70	0.097	0.126
100	0.097	
200	0.099	
300	0.101	
400	0.102	
500	0.102	
600	0.103	
700	0.103	
800	0.103	
900	0.103	
1000	0.104	

Table D-2 presents a comparison on the maximum temperatures using the effective specific heat and density of the homogenized basket listed in Table 4-10 to those listed in Table D-1. As seen from Table D-2, the maximum difference in the DSC shell temperature is 1°F and is negligible. Therefore, the CCNPP-FC TC analysis and the resulting DSC temperature profiles used in the 32PHB DSC/Basket analysis in [13] for the fuel cladding temperatures remain bounding.

Table D-2 Sensitivity of Maximum Temperatures to Effective Density and Specific Heat

Component	Temperature [°F]		
	Off-Normal Hot (Load Case # 6)		Difference
	(Sensitivity Run)	(Original Model, Table 6-1)	$T_{Sensitivity} - T_{Original}$
	time = 20 hr		
Max. DSC Shell	408	407	+1
Inner Shell	314	313	+1
Gamma Shield	308	308	0
Structural Shell	264	263	+1
Bulk Avg. Temp of Radial Neutron Shield	214	214	0
Bulk Avg. Temp of Top Neutron Shield	186	186	0
Bulk Avg. Temp of Bottom Neutron Shield	201	201	0
Cask Lid	217	216	+1
Cask Outer Shell	233	233	0